


A Genuine Interindividual Variability in Number and Anatomical Localization of Face-Selective Regions in the Human Brain

Xiaoqing Gao¹, Minjie Wen², Mengdan Sun¹  and Bruno Rossion^{3,4}

¹Center for Psychological Sciences, Zhejiang University, Hangzhou 310028, China

²Department of Psychology, Zhejiang University, Hangzhou 310028, China

³Université de Lorraine, CNRS, CRAN, F-54000, Nancy, France

⁴Université de Lorraine, CHRU-Nancy, Service de Neurologie, F-54000 Nancy, France

*Address correspondence to Xiaoqing Gao, Center for Psychological Sciences, Zhejiang University, 148 Tianmushan Road, Hangzhou 310028, China. Email: xiaoqinggao@zju.edu.cn; Bruno Rossion, CRAN UMR 7039, CNRS - Université de Lorraine, Pavillon Krug, Hôpital Central, CHRU Nancy, 29 Avenue du Maréchal de Lattre de Tassigny, 54035 Nancy, France. Email: bruno.rossion@univ-lorraine.fr

Abstract

Neuroimaging studies have reported regions with more neural activation to face than nonface stimuli in the human occipitotemporal cortex for three decades. Here we used a highly sensitive and reliable frequency-tagging functional magnetic resonance imaging paradigm measuring high-level face-selective neural activity to assess interindividual variability in the localization and number of face-selective clusters. Although the majority of these clusters are located in the same cortical gyri and sulci across 25 adult brains, a volume-based analysis of unsmoothed data reveals a large amount of interindividual variability in their spatial distribution and number, particularly in the ventral occipitotemporal cortex. In contrast to the widely held assumption, these face-selective clusters cannot be objectively related on a one-to-one basis across individual brains, do not correspond to a single cytoarchitectonic region, and are not clearly demarcated by estimated posteroanterior cytoarchitectonic borders. Interindividual variability in localization and number of cortical face-selective clusters does not appear to be due to the measurement noise but seems to be genuine, casting doubt on definite labeling and interindividual correspondence of face-selective “areas” and questioning their a priori definition based on cytoarchitectony or probabilistic atlases of independent datasets. These observations challenge conventional models of human face recognition based on a fixed number of discrete neurofunctional information processing stages.

Key words: face selectivity; fMRI; human brain; interindividual variability; ventral occipitotemporal cortex.

Introduction

Since the seminal positron emission tomography (PET) study of [Sergent et al. \(1992\)](#), neuroimaging studies carried out for three decades, mainly with functional magnetic resonance imaging (fMRI), have disclosed clusters of voxels with more neural activation to pictures of faces than nonface visual stimuli in the human brain (e.g., [Puce et al. 1995](#); [Kanwisher et al. 1997](#); [Halgren et al. 1999](#); [Ishai et al. 2005](#); [Fox et al. 2009](#); [Weiner and Grill-Spector 2010](#); [Rossion et al. 2012](#); [Zhen et al. 2015](#); [Gao et al. 2018](#); [Schwarz et al. 2019](#); [Finzi et al. 2021](#)). Despite a substantial amount of variability in the paradigms and stimuli used across fMRI studies ([Duncan et al. 2009](#); [Berman et al. 2010](#)), these “face-selective” clusters have been reported in consistent gross anatomical structures across studies, mainly in both the ventral occipitotemporal cortex (VOTC) and the superior temporal sulcus (STS).

The different fMRI-defined face-selective clusters of the human occipitotemporal cortex have been labeled

according to the anatomical region where they are usually disclosed. For instance, the well-known “fusiform face area” (FFA, labeled by [Kanwisher et al. 1997](#)) is a face-selective cluster identified in the middle section of the anterior–posterior axis of the fusiform gyrus, while the “occipital face area” (OFA, labeled by [Gauthier et al. 2000](#)) is typically identified in the lateral section of the inferior occipital gyrus. Following this logic, up to six face-selective clusters, that is, four in the VOTC (OFA, posterior FFA [pFFA], middle FFA [mFFA], anterior temporal lobe face area [ATL-FA]) and two in the STS (posterior [pSTS-FA], anterior [aSTS-FA] STS face area, respectively), have been defined in the most recent neurofunctional model of human face recognition ([Duchaine and Yovel 2015](#); for earlier models, see [Haxby et al. 2000](#); [Calder and Young 2005](#); [Ishai 2008](#); [Rossion 2008](#); [Haxby and Gobbini 2011](#)). These face-selective clusters of voxels are thought to contain populations of (millions of) neurons ([Logothetis 2008](#)), which, by definition, must play

a key role in the recognition of a visual stimulus as a face.¹ Beyond this generic face recognition function, many fMRI studies have tested the sensitivity of these face-selective clusters—in particular the FFA—to physical stimulus manipulations (e.g., position, size, head orientation, and various image statistics; see, e.g., Tong et al. 2000; Levy et al. 2001; Yue et al. 2011; Rice et al. 2014; Finzi et al. 2021), to attention (e.g., O'Craven et al. 1999; Peelen et al. 2009), and conscious perception (e.g., Tong et al. 1998; Andrews et al. 2002; Fang and He 2005), and investigated their putative role in finer grained facial recognition functions (e.g., face familiarity and identity, facial expression, eye gaze direction, etc.; for reviews, see Haxby and Gobbini 2011; Rossion 2014; Duchaine and Yovel 2015; Grill-Spector et al. 2017). Another important line of research focuses on the origin and developmental trajectory of these fMRI face-selective clusters (Golarai et al. 2007, 2015; Scherf et al. 2011).

In these studies, the face-selective cortical clusters are considered to be discrete components, that is, information processing stages, of a well-defined neurofunctional network in the human brain, with a definite pattern of anatomofunctional connectivity (Fairhall and Ishai 2007; Gschwind et al. 2012; Pyles et al. 2013; Frässle et al. 2016; Weiner et al. 2017; Elbich et al. 2019; Wang et al. 2020; Kessler et al. 2021). Comparative studies have also attempted to relate these face-selective neural clusters one-by-one across different species of the primate order (macaques and humans: Tsao et al. 2008; Rajimehr et al. 2009; Yovel and Freiwald 2013; marmosets to macaques and humans: Hung et al. 2015; see Weiner and Grill-Spector 2015).

Overall, the ultimate objectives of this ongoing research program are to 1) define each component of the human cortical face network, 2) determine its anatomical features and intrinsic/extrinsic anatomofunctional connections, and 3) understand the nature of its local representations and processes (Grill-Spector et al. 2017; see also Freiwald 2020 and Hesse and Tsao 2020 in nonhuman primates). For instance, in humans, fMRI studies have associated face-selective regions of the human STS with dynamic aspects of face recognition (e.g., facial expression, eye gaze, and head orientation) whereas those in the VOTC are instead thought to be predominantly involved in more stable aspects of face recognition (e.g., identity, gender, etc.) (Allison et al. 2000; Haxby et al. 2000; Bernstein and Yovel 2015; Duchaine and Yovel 2015; Pitcher and Ungerleider 2021). In both the STS and VOTC pathways, the prevalent view is that of a progressive, hierarchical evolution in the degree of

view invariance and complexity of facial representation from posterior to anterior face-selective regions (e.g., Duchaine and Yovel 2015; Meyers et al. 2015; Weiner et al. 2017; Tsantani et al. 2021).

A key assumption of this research study is therefore that all neurotypical adult individual brains hold the same number of neurofunctional clusters/regions, with each region restricted to one cytoarchitectonic area (Weiner et al. 2017), and with the set of regions organized along the same pattern of anatomofunctional connectivity (i.e., a general “face connectome”; Wang et al. 2020). Based on this assumption, probabilistic atlases are being increasingly developed to define these face-selective clusters/regions in a new individual brain based on its cortical anatomy and using functional data collected on an independent set of typical participants (Julian et al. 2012; Engell and McCarthy 2013; Rosenke et al. 2021).

However, although there are undoubtedly large-scale anatomical constraints common to all individual brain for the localization of face-selective clusters (e.g., in the lateral rather than the medial section of the fusiform gyrus, Weiner and Grill-Spector 2010, 2012; Weiner et al. 2017; Margalit et al. 2020; see also Jonas et al. 2016; Hagen et al. 2020 for intracerebral recording evidence), there is also a sheer amount of variability in terms of level of face selectivity, size, and anatomical localization of these fMRI clusters across individual brains (Rossion et al. 2012; Zhen et al. 2015; Schwarz et al. 2019). Interindividual variability in volume and/or level of face selectivity of some of these clusters has been well acknowledged from the outset (e.g., Kanwisher et al. 1997; Rossion et al. 2003; Gauthier et al. 2005; Pinsk et al. 2009) and sometimes even successfully correlated with behavioral performance at face identity recognition (Jiang et al. 2013; Huang et al. 2014; Weibert and Andrews 2015; Elbich and Scherf 2017; Hermann et al. 2017; McGugin et al. 2018). Interindividual variability of peak location of face-selective clusters, often the FFA and OFA, is also well known, ranging from several millimeters to centimeters (Kanwisher et al. 1997; Rossion et al. 2003; Fox et al. 2009; Pinsk et al. 2009; Pitcher et al. 2011; Rossion et al. 2012; Zhen et al. 2015; Schwarz et al. 2019).

To our knowledge, a potentially genuine interindividual variability in terms of the “number” of face-selective clusters in the human brain has only been raised in one large-scale ($n=40$) fMRI face localizer study (Rossion et al. 2012). The following study of Zhen et al. (2015), performed on 202 participants, reported a large amount of variability in anatomical localization of face-selective clusters but, in contrast, a fixed number (6) of face-selective clusters that were searched for in each individual brain. Hence, even in a study that addressed and emphasized interindividual variability in anatomical localization of face-selective clusters, the number of face-selective clusters across individuals was held constant a priori, as in all other fMRI face localizer studies investigating the whole cortical face network (e.g., Wang et al. 2020). This approach is not surprising because

¹ In psychology, the term “recognition” often implies a judgment of previous occurrence [specifically “the ability to identify information as having been encountered before,” APA Dictionary of Psychology; see also Mandler 1980]. However, the term is used here in a general biological meaning to refer to the production of a selective [i.e., discriminant] response to a given sensory input, a response that can be reproduced [i.e., generalized] across variable viewing conditions. As defined, face recognition is essentially the same function as face categorization [Rossion and Retter 2020], and the two terms are used interchangeably in this article.

authentic interindividual variability in terms of the number of face-selective clusters in the human brain would pose a substantial challenge for neurofunctional models of human face recognition (and systems neuroscience in general). That is, if neurotypical individual brains truly have different numbers of face-selective clusters, spanning over different cytoarchitectonic brain areas, how could one generalize across individual brains to precisely define the nature of representations and processes performed in each of these “components” and relate them intelligibly in a generic neurofunctional architecture?

The present fMRI study focuses on this issue of interindividual variability in terms of anatomical localization and spatial extent/distribution of face-selective clusters and, especially, in terms of their number in the human occipitotemporal cortex and STS. Its major goal is to describe and quantify this variability and assess whether it is real or if it is rather due to measurement noise. To do that, a relatively large sample of participants for assessing and visualizing interindividual variability ($n=25$) was tested with a face localizer fMRI experiment recently developed and validated with a smaller sample (Gao et al. 2018; see also Gao et al. 2019). The paradigm used to localize face-selective clusters relies on the presentation of a large set of natural (i.e., unsegmented) and highly variable images of nonface stimuli of multiple living and nonliving categories at a fast (6 images/s, 6 Hz) periodic rate, with “mini-bursts” of natural images of faces appearing every 9 s, that is, at 0.111 Hz (Fig. 1A). A large set of natural images of faces varying in size, luminance, contrast, head orientation, lighting conditions, gender, expression, etc. (Fig. 1A) is used to ensure that selective neural responses to the category of faces are not due to low-level visual cues (i.e., low-level image statistics contained in the amplitude spectrum of the images, or specific local features such as the hairline contrast or the same features falling in the same positions as with homogenous segmented stimulus sets).

As this frequency-tagging paradigm provides objectivity to identifying significant neural activity (i.e., at a pre-defined frequency; Fig. 1B), high sensitivity (i.e., signal-to-noise ratio, SNR), and high test-retest reliability (80–90%) to disclose face-selective neural activity in the human occipitotemporal cortex (Gao et al. 2018), it is ideal to fully address the issue of interindividual variability in anatomical localization and number of cortical face-selective clusters in the human brain. Across the 25 participants tested with this paradigm, the mean and standard deviation of the activated volume, maximum SNR, number of face-selective clusters and number of local maxima were defined here for four anatomically defined regions-of-interest (ROIs): the lateral occipital (LO) cortex, middle fusiform (midFus) cortex, anterior temporal lobe (ATL), and posterior STS (pSTS) (see [Materials and Methods](#)). Although the cortical gray matter distance can be underestimated with volume-based rather than cortical surface visualizations in individuals

(Weiner and Grill-Spector 2011), face-selective clusters were defined in original volumetric space rather than in a surface-based space to prevent any potential artificial dissociation of clusters in the process of mapping from volumetric space to surface space. Importantly, spatially unsmoothed data was used in order to prevent artificially merging individual clusters as a result of smoothing (e.g., Weiner and Grill-Spector 2012), thereby preserving potential interindividual variability.

With this approach, we report a large amount of interindividual variability in spatial extent, distribution, and number of face-selective clusters in the VOTC and STS regions. As across individuals the number of clusters is not related to the total face-selective volume activated, maximal SNR, or statistical threshold used, our data suggest that this interindividual variability is genuine. Although face-selective clusters in the VOTC are largely confined to the lateral rather than the medial fusiform gyrus in line with previous observations (Weiner and Grill-Spector 2012; Weiner et al. 2017), there is no systematic association between atlas-based cytoarchitectonic regions and face-selective clusters in the posteroanterior axis. These observations have important implications for investigating and understanding the neural basis of human face recognition.

Materials and Methods

Participants

We collected fMRI data from a total of 25 adult participants (16 female, mean age = 30 ± 5.7 years, age range = 21–44 years), among whom 15 were tested at York University, Canada, and 10 were tested at Maastricht University, the Netherlands. Data of a subset of participants ($n=12$) were reported in a previous methodological work demonstrating the high sensitivity, specificity, and reliability of the fMRI “face localizer” used (Gao et al. 2018). All the participants had normal or corrected-to-normal vision and were right handed (Oldfield 1971). None of the participants reported any history of psychiatric or neurological disorders or current use of any psychoactive medications. The study was approved by York University Research Ethics Board and the Ethical Committee of the Medical Department of the University of Louvain, Belgium. We obtained informed written consent from all the participants prior to the experimental sessions, and the participants received monetary compensation for their participation in the study.

Stimuli

As in Gao et al. (2018), the stimuli consisted of 100 face images and 200 nonface images. The face images were digital photographs of 100 different individuals who were nonfamous relatives, friends, and colleagues of the researchers of the Face Categorization Lab then at the

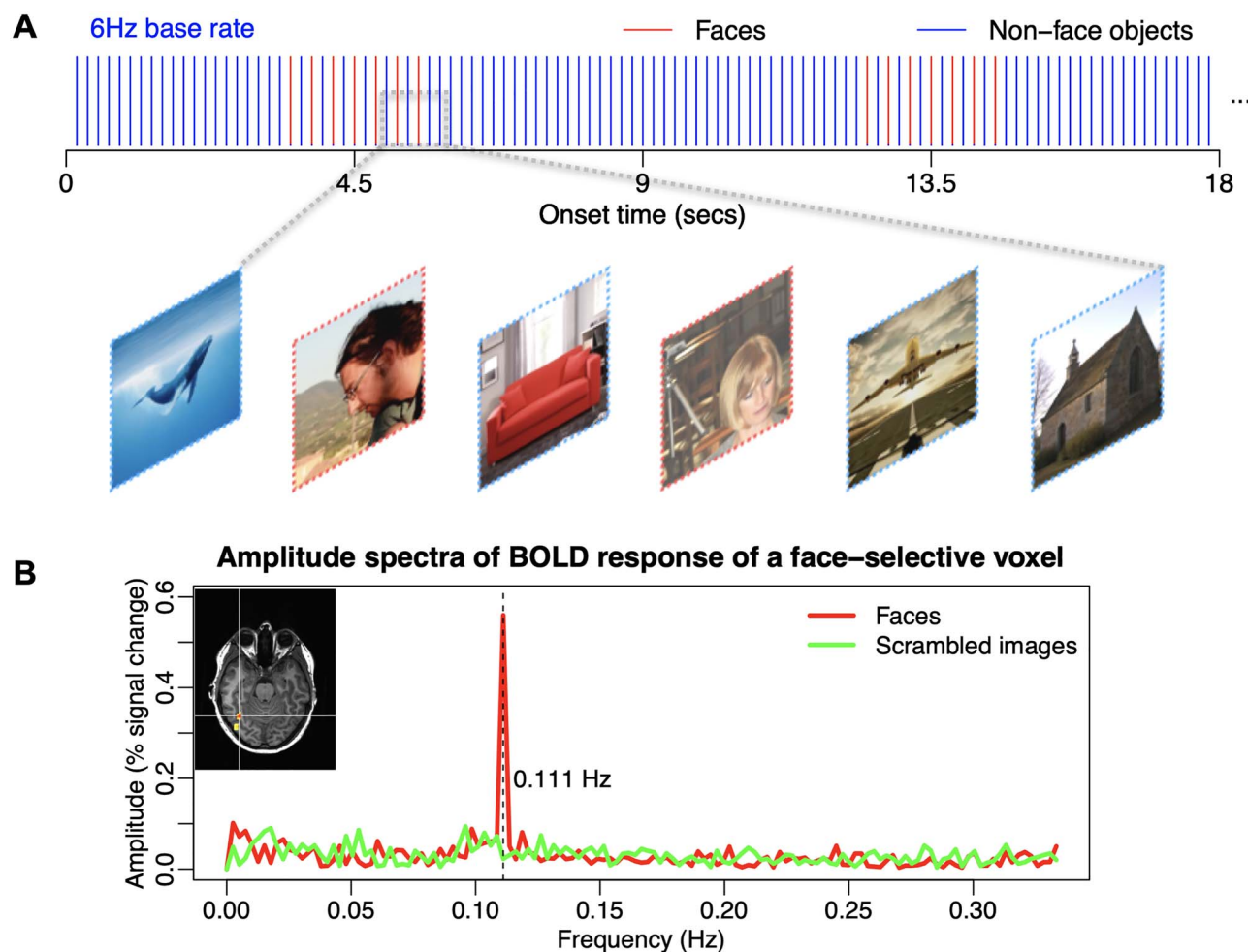


Figure 1. Experimental paradigm (from Gao et al. 2018). (A) During the scanning run, variable natural images of nonface stimuli are presented at a fast rate of 6 Hz (6 images/s). Every 9 s (0.111 Hz), a “mini-burst” of 7 highly variable face images alternates with nonface images, covering a period of 2.167 s. This procedure prevents category-based adaptation effects within a mini-block and, with a stimulus-onset asynchrony of 333 ms between two faces, allows capturing the bulk of every underlying face-selective response (Retter and Rossion 2016). These two factors contribute to the high signal-to-noise ratio of the face-selective activation observed with this approach (Gao et al. 2018). The frequency of face bursts (0.111 Hz) is referred to as the face stimulation frequency with a signal at 0.111 Hz in the fMRI spectrum, reflecting face-selective activity. (B) In one example brain, the highest face-selective activity at 0.111 Hz as found in the right lateral middle fusiform gyrus, with no increased 0.111 Hz activity to the same images matched for low-level properties (amplitude spectrum) but phase-scrambled to prevent face or object recognition.

University of Louvain in Belgium. Therefore, they were unfamiliar to the participants. Each photograph contained one human face. The photographs were originally taken for personal purposes and were given to the researchers with a completed consent form to use these photographs for research purposes and display them. They contain a natural range of variation in size, pose, and expression of the faces depicted in the photographs and in lighting and background. The nonface images consist of 200 photographs of scenes, objects, and animals. As in the face images, the nonface images also contain a natural range of variation in the composition and lighting of the images. The face images have a mean grayscale intensity value of 115.0 ± 1 and a mean contrast value of 0.49 ± 0.11 . The nonface object images have a mean grayscale intensity value of 115.2 ± 0.9 and a mean contrast value of 0.46 ± 0.12 . On average, there is no statistical difference between the two sets of images on either the grayscale intensity value ($t_{298} = 1.8$, $P = 0.068$,

two-tailed) or the image contrast ($t_{298} = 0.7$, $P = 0.49$, two-tailed).

The images were back-projected in full color onto a projection screen by an MRI compatible LCD projector and viewed by the participant through a mirror placed within the RF head coil at a viewing distance of 43 cm (York University) or 75 cm (Maastricht University). They extended the same visual angle (14.6×14.6 degree) at both viewing distances (or 11×11 cm on the screen at York University and 19.2×19.2 cm at Maastricht University). The remaining area of the screen was set to a uniform gray background. The whole experiment procedure was controlled through a stimulation program running in Java, which also collected behavioral responses.

FMRI Paradigm

We used the same fMRI paradigm as described in Gao et al. 2018. The images were displayed at a base rate of 6 Hz (i.e., 6 images/s, Fig. 1A), thus with a stimulus

onset asynchrony (SOA) of 166.7 ms (10 screen refresh cycles at a refresh rate of 60 Hz), allowing only one gaze fixation per image. Images were contrast modulated by a sinusoidal function so that each image appeared at 0% contrast, reached 100% contrast at the sixth frame and then dropped its contrast to 9.55% at the 10th frame. Every 9 s, a set of 7 faces (referred to as a “mini-burst,” covering 2.167 s, the red bins in Fig. 1A) appeared at a rate of 3 Hz, that is, alternating with nonface images (blue bins in Fig. 1A). Each run had a length of 396 s so that the mini-burst appeared 44 times at a fixed frequency of 1/9 Hz (i.e., 0.111 Hz, referred to as the face stimulation frequency). For each presentation, an image was drawn from the corresponding image set (face or nonface) according to a random order. When all the images in the respective sets had been presented, a new random order was generated and the images were drawn according to this new random order.

Behavioral Task

Participants performed a behavioral task, orthogonal to the measure of interest. They were instructed to press a predefined key on an MRI compatible response pad using the right index finger when they detected color changes of the central crosshairs (+) superimposed on the images (Rossion et al. 2015; Gao et al. 2018). The crosshairs extended a visual angle of 1.2 degrees in the center of the screen. During each run, the color of the crosshairs changed from black to white for 200 ms, for a total of 70 times with the interval between two changes randomized while keeping above a minimal interval of 2 s. All participants achieved high accuracy (mean accuracy = $91.2\% \pm 2.0$) in the behavioral task.

MR Image Acquisition

For participants at York University, we acquired the MRI images using a 3 T Siemens Magnetom Trio system (Siemens Medical System) with a 32-channel head coil. Anatomic images were collected using a high-resolution T1-weighted magnetization-prepared gradient-echo image (MP-RAGE) sequence (192 sagittal slices, TR = 2300 ms, TE = 2.62 ms, voxel size = 1 mm isotropic, FA = 9°, FoV = $256 \times 256 \text{ mm}^2$, matrix size = 256×256 , parallel scanning mode = GRAPPA, accelerate factor = 2). Functional images were collected with a T2*-weighted gradient-echo echoplanar imaging (EPI) sequence (TR = 1500 ms, TE = 30 ms, FA = 62°, voxel size = 3 mm isotropic, FoV = $192 \times 192 \text{ mm}^2$, matrix size = 64×64 , interleaved, parallel scanning mode = GRAPPA, accelerate factor = 2), which acquired 25 oblique-axial slices covering the whole occipital lobe and the whole temporal lobe. For participants at Maastricht University, we acquired the MRI images using a 3 T Siemens Magnetom Prisma scanner (Siemens Medical System) with a 64-channel head-neck coil. Anatomic images were collected using a high-resolution T1-weighted magnetization-prepared gradient-echo image (MP-RAGE) sequence (192 sagittal slices, TR = 2250 ms,

TE = 2.21 ms, voxel size = 1-mm isotropic, FA = 9°, FoV = $256 \times 256 \text{ mm}^2$, matrix size = 256×256). Functional images were collected with a T2*-weighted gradient-echo echoplanar imaging (EPI) sequence (TR = 1500 ms, TE = 30 ms, FA = 72°, voxel size = 3-mm isotropic, FoV = $240 \times 240 \text{ mm}^2$, matrix size = 64×64 , interleaved), which acquired 23 oblique-axial slices covering the whole occipital lobe and the whole temporal lobe. In both scanners, each functional run took 414 s. All 25 participants performed at least two scanning runs, and a subset of participants ($n = 13$) who were not involved in another fMRI experiment subsequently performed an additional run of the face localizer.

Data Analysis

Preprocessing

The functional runs were motion-corrected in reference to the average image of the first functional run of the experiment using a 6° rigid body translation and rotation via an intra-modal volume linear registration using the FMRIB software library (FSL, version 5.0.8, Smith et al. 2004). We then removed linear trends from the preprocessed time series data of each voxel and converted the time series data to percentage of blood oxygen level-dependent (BOLD) signal change by dividing the time series of each voxel by its mean signal intensity. No spatial smoothing was performed on the data.

SNR of the Face-Selective Response

As in Gao et al. (2018), for each scanning run, we performed fast Fourier transform (FFT) to obtain the amplitude spectrum of the BOLD response time series. To gauge the strength of the BOLD response at the face stimulation frequency (the signal) relative to the noise, we converted the amplitude of the face stimulation frequency (0.111 Hz) to a Z-score as in previous studies (McCarthy et al. 1994; Puce et al. 1995). Intrinsically, a z-score is a measure of SNR. Therefore, we referred to the Z-scores to as SNR of the face-selective neural responses:

$$\text{SNR} = (A_s - \mu_N) / \sigma_N, \quad (1)$$

where A_s is the amplitude of the face stimulation frequency, μ_N is the mean and σ_N is the standard deviation of the amplitude of 40 neighboring frequencies (20 on each side, e.g., Rossion et al. 2015, Jonas et al. 2016). This procedure is applied to each voxel independently. Across runs, the responses to the periodic face stimulations in a given population of neurons have the same phase, while any noise from a periodic source (e.g., pulse, breathing) could have different phases. Therefore, we averaged the time series across scanning runs to increase the signal-to-noise ratio, similarly to the use of this approach in electrophysiology (Regan 1989). The averaged time series across runs was submitted to the same calculation as with the data from individual runs. This analysis is performed with custom code based on Matlab (Mathworks).

The code and example data are publicly available on https://www.nitrc.org/projects/fpsfmri_face/.

Defining Activation and Deactivation of Neural Responses

As in Gao et al. (2018), we defined the activation and deactivation of the neural response using the phase of the BOLD response at the stimulation frequency. In general, a positive phase value indicates an increasing BOLD response amplitude after the onset of the face stimuli, whereas a negative phase value indicates a decreasing BOLD response amplitude after the onset of the face stimuli. To account for individual differences in the time to reach maximum BOLD response amplitude, for each individual we calculated the histogram (20 bins) of phase values of all the voxels with a criterion of z -score > 3 and with a positive phase value. We used the phase value of the histogram bin that has the largest number as the center phase (φ) and defined all the voxels with their phase values within $\varphi \pm \pi/2$ as activations (+ sign) and voxels with their phase values outside of this window as deactivations (− sign). We then applied the signs to the SNR (Z -score) maps and obtained the final response map containing only voxels that have increased BOLD response (+ sign) to the presence of the target stimuli.

Criteria for Defining Face-Selective Voxels

Given the high sensitivity of the paradigm and the objectives of the study, we deliberately used a conservative two-step criterion to define face-selective voxels. In the first step, we selected the voxels that are consistently above a threshold level in each scanning run. For participants who performed three scanning runs ($n=13$), we used a threshold level of ($Z > 1.2816$), so that the joint probability of having all three runs greater than the threshold at a given voxel is $P < 0.001$. For participants who performed two scanning runs ($n=12$), we used a threshold level of ($Z > 1.8575$), so that the joint probability of having both runs greater than the threshold at a given voxel is also $P < 0.001$. We define the voxels that are selected by the first step as the “consistent voxels.” In the second step, within the consistent voxels, we further selected voxels above a threshold of ($Z > 3.719, P < 0.0001$), based on the SNR values calculated from the run-averaged time series. We estimated the false discovery rate by applying the above criteria to SNR values calculated for two noise frequencies (± 2 of the target frequency). On average, at the noise frequencies, the false discovery rate is of 0.001 ± 0.0012 . Hence, we are confident that truly face-selective voxels were selected, avoiding an overestimation of the number of face-selective clusters in individual brains.

Cluster Analysis

We identified face-selective clusters of voxels that are connected to each other by at least a corner, with a minimal volume of 81 mm^3 (3 voxels at the size of $3 \times 3 \times 3 \text{ mm}^3$) in volumetric space. We compared the clusters identified by the volumetric clustering to

clusters identified by surface-based cluster analysis with the volumetric functional data projected onto individual cortical surface (using Freesurfer). As projecting volumetric data to cortical surface can artificially separate a single cluster in volumetric space to different clusters in the cortical surface (Supplementary Fig. 1), clustering in volumetric space appears to capture the number of clusters more accurately than surface-based clustering (Supplementary Table 1). To gauge how reliable these face-selective clusters are, we calculated the Dice Coefficient between the voxels in these face-selective clusters within the anatomically defined Fusiform gyrus and all the face-selective voxels in each individual scanning runs within the same ROI with a conservative threshold of ($Z > 3.719$). On average, we achieved a Dice Coefficient of 0.81 ($SD=0.12$, with a 3-mm FWHM smoothing, as in Gao et al. 2018) or 0.77 ($SD=0.11$, without spatial smoothing). Therefore, the face-selective clusters identified here are highly reliable.

Identifying Local Maxima

Within the face-selective clusters defined in the above step, we identified local maxima with a minimal Z -score of 5 and a minimal separation distance of 10 mm from other local maxima. Finding more than one local maxima in the same cluster suggests that, with a higher threshold (or alternatively, a less sensitive face localizer paradigm) a continuous cluster may be identified as several clusters. At the same time, as the threshold for defining local maxima ($Z \geq 5$) is higher than the threshold for defining clusters ($Z > 3.719$), there could be cases of no local maxima within a face-selective cluster.

Anatomical ROIs

For each individual brain, we labeled cortical regions using an automated algorithm as part of the Freesurfer processing pipeline. This algorithm defines the cortical areas based on folding patterns and has been validated to have high accuracy (Destrieux et al. 2010). From the resulting labels generated by Freesurfer, we combined the fusiform gyrus (G_occipit-temp_lat-Or_fusiform) and fusiform sulcus (S_occipitotemporal_lateral) from the automated labels to form a fusiform ROI. We combined the anterior occipital sulcus (S_occipital_anterior), inferior occipital gyrus (G_and_S_occipital_inferior), middle occipital gyrus (G_occipital_middle) and sulcus (S_occipital_middle_and_Lunatus) to form a lateral occipital ROI. We selected the automatically labeled superior temporal sulcus (S_temporal_superior) as the STS ROI. We defined an anterior/posterior boundary as the posterior end of the hippocampus (Kim et al. 2000). Based on this anterior/posterior boundary, the fusiform ROI and the STS ROI are both divided into an anterior part and a posterior part. We further combined the anterior fusiform with an automatically labeled anterior OTS (S_collateral_transverse_ant as defined in the atlas, but it is the OTS) and the temporal pole (Pole_temporal) to form an ATL ROI. Therefore, for each individual brain,

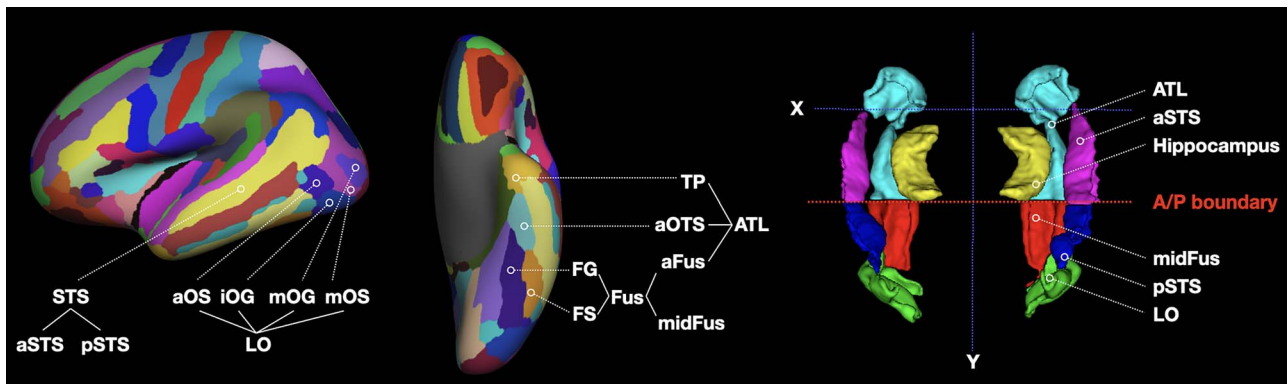


Figure 2. ROIs defined based on automatic algorithms using the surface folding pattern (Freesurfer). The anterior/posterior boundary was defined as the posterior end of the hippocampus (Kim et al. 2000). Left: Automatically labeled cortical areas based on folding pattern by Freesurfer. Right: The four ROIs selected for the current study: Anterior temporal lobe (ATL), posterior STS (pSTS), middle fusiform (midFus), and lateral occipital (LO).

within each hemisphere, we defined four ROIs: lateral occipital (LO), middle fusiform (midFus), ATL, and pSTS (Fig. 2).

Complementary Study: Face- and Limb-Selective Activity

To test the possibility that the spatial organization of face-selective clusters identified with the present face-localizer paradigm could be due to or modulated by selective neural activity to nonface body parts (Weiner and Grill-Spector 2010), we ran an additional experiment comparing face-selective clusters and limb-selective clusters in a small group of participants ($n=4$). In brief, each participant performed a face-localizer task (2 runs) and a limb-localizer task (2 runs), with the same procedure as in the main experiment (see [Supplementary Methods](#) for details). We identified face- and limb-selective clusters of voxels with the same criterion ($Z>3.719$, cluster size $>81 \text{ mm}^3$) as in the main experiment, and defined the face-selective clusters within the anatomically defined lateral occipital ROI and fusiform ROI with all the voxels that overlap with significant limb-selective voxels removed.

Results

Group Averaging Reveals Large-Scale Anatomical Constraints of Face-Selective Activation

First, we describe the group averaged face-selective activations and relate them to typical regions reported in the literature. To provide a first overview of interindividual variability/consistency in localization of neural activity, we also report the degree of overlap in statistical significance at the voxel level among individual participants. To do so, we averaged the binarized activation maps across individual brains using a surface-based intersubject coregistration procedure, and displayed the activation probability map on an averaged cortical surface of all the participants (Fig. 3A). The resulting activation probability map shows that face-selective activation is both confined and extended at a group level, that is, it concerns essentially along the ventral and dorsal surface

of the LO cortex, ventrally running anteriorly along the lateral fusiform gyrus, and dorsally onto the pSTS. The highest activation overlap at the voxel level reached 0.88 (22 out of 25 participants), with 55 voxels (1 mm^3 isovoxel) in the right middle fusiform gyrus above an overlap index of 0.8. With a cut-off activation probability of 0.12 (i.e., 3 of 25 participants; as reference, a cut-off of 0.1 was used in Zhen et al. 2015), there is no break in the pSTS-LO-Fusiform continuum. However, ventrally, the middle fusiform sulcus serves as a sharp boundary, where the activation is confined to the lateral side of the fusiform gyrus without extending into the medial side (Fig. 3A). This finding is fully consistent with proposal that the middle-fusiform sulcus is an anatomical boundary of face-selective activation (Weiner and Grill-Spector 2012; Weiner et al. 2017; Weiner 2019). The same pattern is observed in the left hemisphere (Supplementary Fig. 2).

The distribution of the individual local maxima (Fig. 3B) follows a similar pattern as seen in the activation probability map. The local maxima are distributed in the same pSTS-LO-fusiform continuum, without any obvious break within this continuum. Within the fusiform gyrus, most of the local maxima are located on the lateral side, following along the middle fusiform sulcus as a sharp boundary. Both the activation map and the distribution of the local maxima show a drop in the anterior temporal lobe, between the anterior portion of the fusiform gyrus and the temporal pole (Fig. 3C). This drop is likely to be a result of the characteristic signal drop out in the anterior portion of the ventral temporal lobe due to magnetic susceptibility artifacts (Wandell 2011; Axelrod and Yovel 2013; see Rossion et al. 2018). In sum, the group average analysis confirms that the middle fusiform sulcus serves as a lateral-medial anatomical boundary of face-selective activation (Weiner and Grill-Spector 2012; Weiner et al. 2017). However, at the group level, there is no obvious anterior-posterior anatomical boundary in the pSTS-LO-fusiform continuum for either the activation probability map or the distribution of individual local maxima. In the current study, the surface-based intersubject coregistration procedure yielded an excellent correspondence

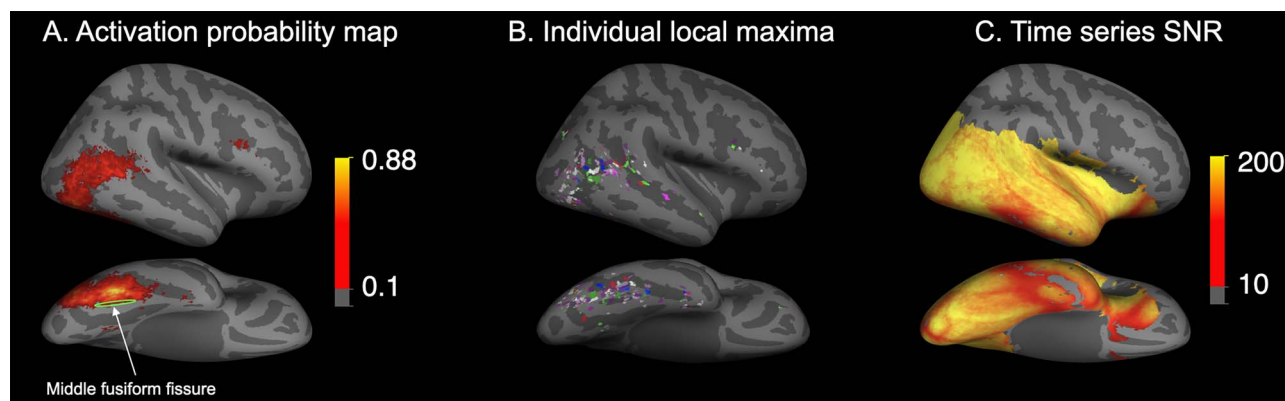


Figure 3. An inflated cortical surface of the averaged right hemisphere showing: (A) the activation probability map in terms of overlap across individual brains (plotted from 0.12 = a voxel activated in 3/25 subjects, to 0.88 = 22/25 individuals). For each individual brain, activation was binarized with a threshold of $Z > 3.719$ ($P < 0.0001$, uncorrected). A surface-based intersubject coregistration procedure was used to create a group-average activation probability map with a cut-off probability of 0.1. (B) Individual local maxima (defined with $Z \geq 5$, minimal separation distance = 10 mm) mapped to the averaged cortical surface of all the participants with a surface-based intersubject coregistration procedure. Individual participants are color-coded, so that all clusters of a given participant are in the same color. (C) The averaged time series signal-to-noise ratio across all participants displayed on the averaged cortical surface. A typical signal dropout is seen in the ventral surface of the anterior temporal lobe.

among individual brains, with the highest activation probability reaching 0.88 even on nonsmoothed data. However, the continuous pattern of activation seen in the pSTS-LO-fusiform cortices could be due to—or increased by—the interindividual variation in brain anatomy and variation in localization of face-selective regions along with averaging. Therefore, further investigation on the localization and extent of face-selective activation at the individual brain level is required.

Number and Size of Face-Selective Clusters in Individual Brains

For each individual brain, with all the face-selective voxels that are above a threshold of $Z > 3.719$ (uncorrected $P < 0.0001$), we ran a cluster analysis (3dclusterize, AFNI) to identify voxels that are connected to each other by at least a corner, with a minimal cluster volume of 81 mm³ (3 voxels at the size of $3 \times 3 \times 3$ mm³). Figure 4 shows all the face-selective clusters within the VOTC of the right hemisphere for each of the 25 participants. While there is some degree of consistency across the majority of participants at a gross anatomical level (e.g., the location and extent of the largest cluster as represented in blue in Fig. 4), there is a substantial amount of variability in number and size of face-selective clusters. Among the 25 individual brains, the number of face selective clusters in the right VOTC varies from 1 to 7 (Fig. 5), with a mode of 3 (mean = 3.4 ± 1.7). Besides variability in the number of clusters, there is also a substantial amount of variability in the composition of clusters across individuals (Figs 4 and 5). In some individual brains, there is a large main cluster in the VOTC spanning across the lateral occipital cortex and the fusiform gyrus (e.g., S05, S07, S10, S20). At the same time, other individual brains have several small clusters scattered in the VOTC (e.g., S03, S09, S22). While the total volume of face-selective clusters in the right VOTC varies substantially across individuals (Fig. 5),

the number of face-selective clusters does not covary significantly with the total volume of face-selective clusters in the VOTC ($r(25) = 0.34$, $P = 0.09$).

For most individual brains, it is difficult, if not impossible, to fit the face-selective clusters into the common scheme of one OFA/IOG and one or two FFAs (pFus and mFus, according to the terminology of Weiner and Grill-Spector 2010; or pFus-faces and mFus-faces; see Grill-Spector et al. 2017) in the VOTC. Importantly, this is not due to spatial smoothing (blurring the boundary between well-defined clusters) because the data was not spatially smoothed in the current study. Also, our observation is not due to the use of a liberal statistical threshold, as we first selected voxels that are consistently activated across multiple runs and applied a relatively conservative threshold ($Z > 3.719$, $P < 0.0001$, uncorrected) compared with the commonly used thresholds in other fMRI face localizer studies (e.g., $Z = 2.3$, $P = 0.01$, uncorrected in Zhen et al. 2015; $P < 0.002$, uncorrected in Weiner and Grill-Spector 2010; $P < 0.001$, uncorrected, in Ishai et al. 2005). Such a two-step procedure to identify face-selective voxels, while being conservative, ensured high reliability. The difficulty to assign these face-selective clusters to an OFA and to an FFA, or to three well-defined clusters (IOG-faces; pFus-faces, mFus-faces), lies on two aspects. First, in some individual brains, a single large cluster accounts for more than 80% of the activated volume in the VOTC and spans across the middle fusiform gyrus and the lateral occipital cortex (Figs 4 and 5; e.g., S06, S07, S10, S13, S16, S17, S20, S24). As there are usually several local maxima within a cluster (Fig. 5), raising the threshold value in such cases would lead to a breakdown into smaller clusters. However, objectively assigning the new clusters to well-defined OFA and FFA or IOG-faces, pFus-faces, and mFus-faces would be impossible (Supplementary Fig. 3).

For most of the individual brains, within each of the anatomically defined lateral occipital cortex and

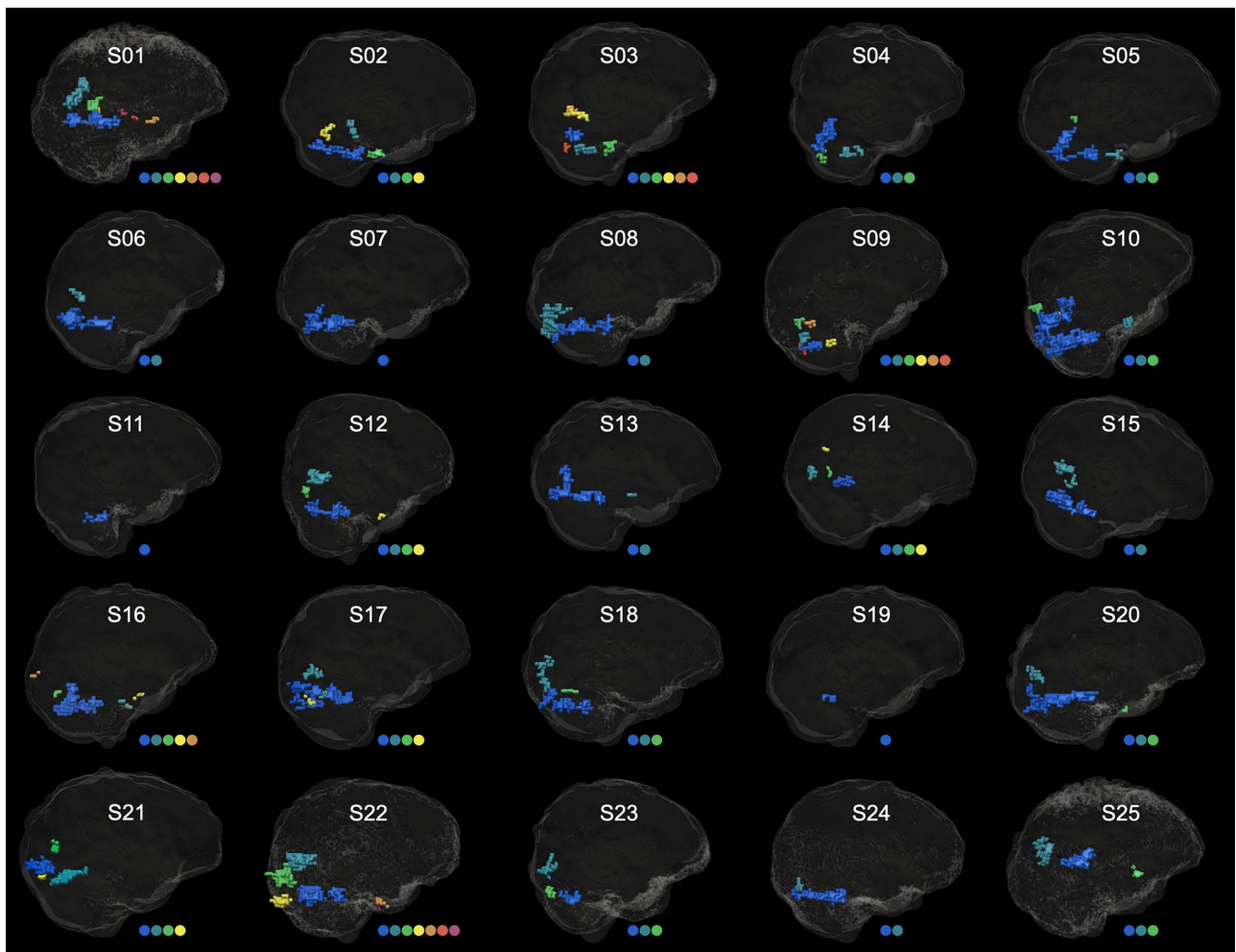


Figure 4. Variability in the number and spatial extent of face-selective clusters in the right ventral occipitotemporal cortex (VOTC) across all 25 participants. The number of clusters varies between 1 (e.g., S07; S11; S19) and 7 (S01, S22). All the clusters are displayed within a VOTC mask (VOTC = LO + midFus + ATL, see [Materials and Methods](#) for the definition of the ROIs). Different clusters are coded by different colors, and the number of clusters in each individual brain is represented by the number of dots below each glass brain. Individual brains are in their native space, aligned to the AC-PC plane.

posterior fusiform gyrus in the right hemisphere, there are more than one cluster (up to 5 clusters in LO and up to 2 clusters in the posterior fusiform gyrus, [Fig. 5](#)) at the current threshold level. Besides, variability in the number of face-selective clusters is also observed in the ATL ROI and the pSTS ROI ([Fig. 5](#)). In [Figure 5](#), we also marked the number of local maxima as defined with $Z \geq 5$, and with a minimal separating distance of 10 mm. If the threshold is raised to a level of $Z = 5$, clusters should center around these local maxima, leading again to a substantial amount of variability in the number of clusters across individual brains. Hence, interindividual variability across brains in terms of number of clusters does not appear to result from the particular threshold used in the main analysis ($Z > 3.719$).

With the same statistical threshold applied to different individual brains, variability in the total volume of face-selective clusters is always expected ([Rossion et al. 2012](#)). Alternatively, a fixed volume of face-selective voxels can be set for all individual brains. By varying the threshold level for individual brains (an average threshold of

$Z = 11.8 \pm 3.6$, range = 4.2–19.5), we selected the top voxels (with the highest face-selective SNR), consisting of a fixed volume of 1000 mm³ in the right hemisphere for each individual. Even with this fixed volume, there is still substantial variability in the number of face-selective clusters, with on average more than one cluster in the LO and in the middle fusiform gyrus ([Fig. 6](#)). At an individual level, in the ATL and pSTS ROIs, even with only the top voxels, there are still cases with two face-selective clusters within each ROI.

Localization of Face-Selective Voxels in Individual Brains

Even at an individual level, face-selective activation falls consistently on the lateral rather than the medial side of the fusiform gyrus ([Fig. 7](#)). However, on the anterior/posterior axis along the ventral surface of the temporal lobe, the localization of face-selective activation varies substantially across individual brains. To quantify the variation in the localization of face-selective voxels along the anterior/posterior axis, we normalized all

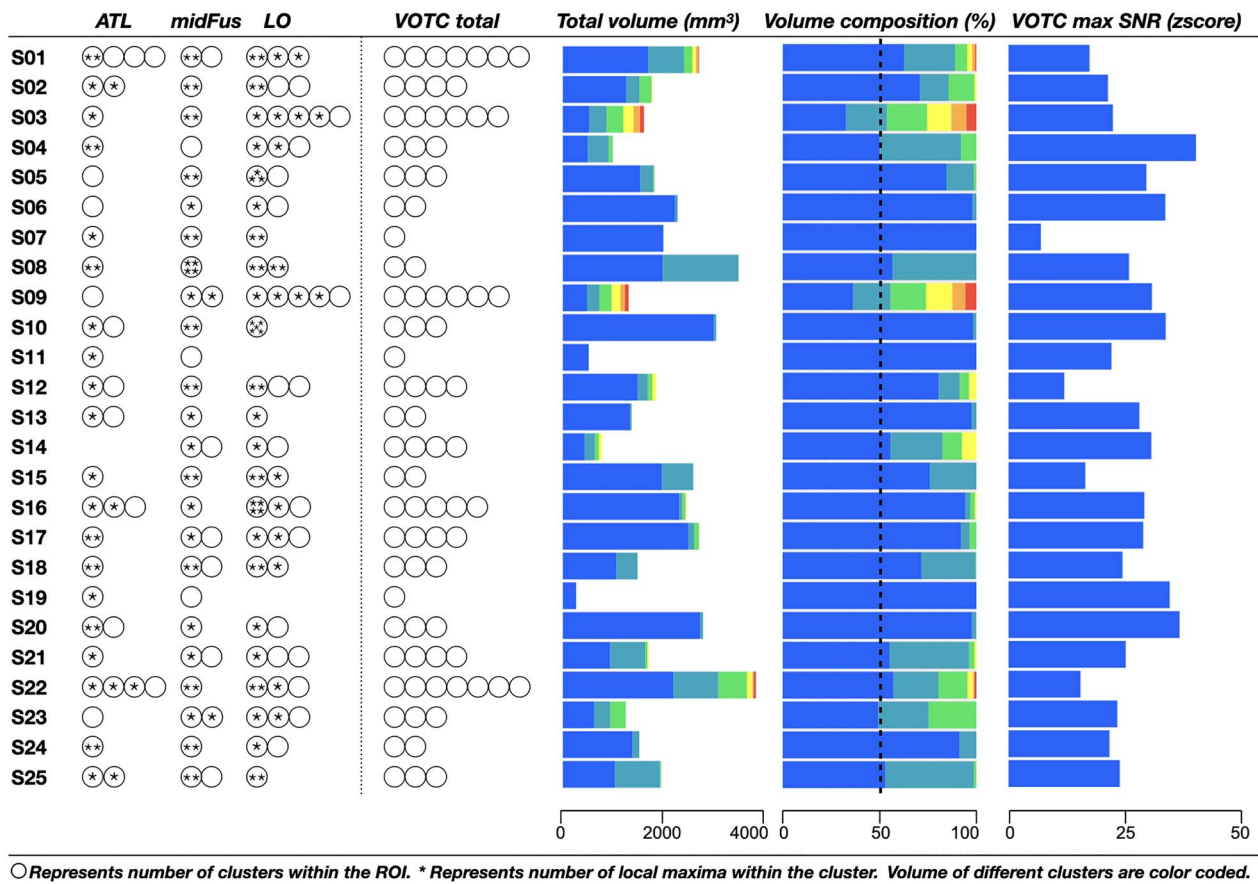


Figure 5. Number and size of face-selective clusters in anatomically defined ROIs in the right ventral occipitotemporal cortex (VOTC). The VOTC consists of three ROIs: ATL, midFus, and LO. Within the VOTC, we also plotted the volume of each cluster (coded by color) and the volume composition (percentage) of each cluster. As local maxima were defined with a higher threshold ($Z \geq 5$) than the threshold used to define clusters ($Z > 3.719$), there could be clusters without any local maxima.

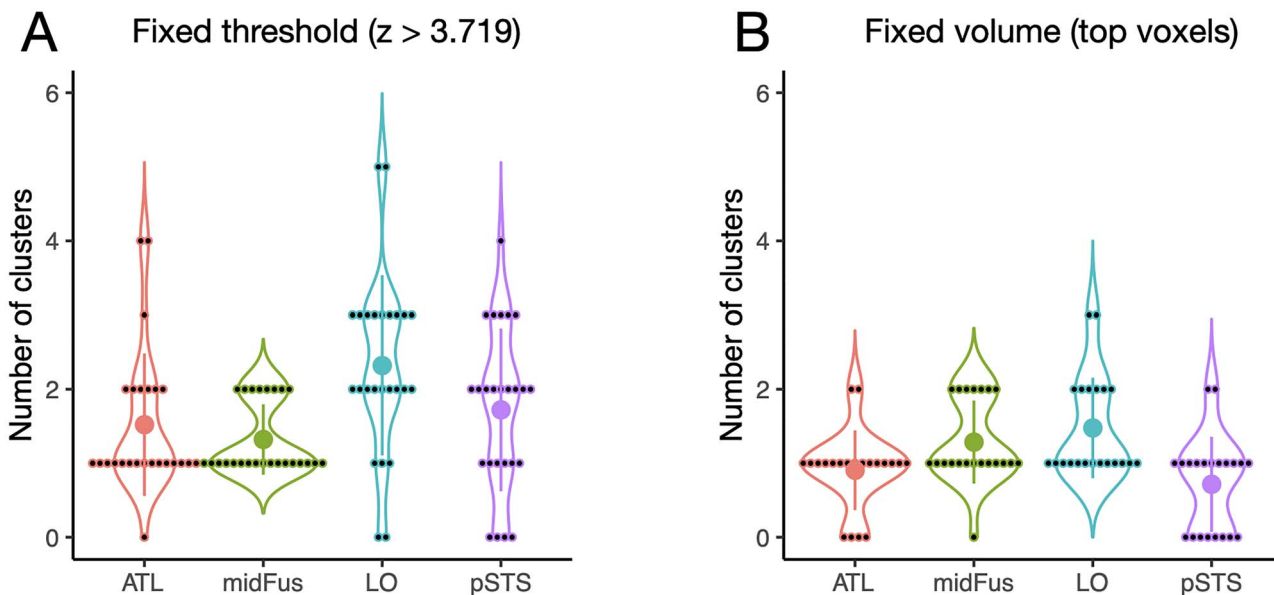


Figure 6. Violin plots showing: (A) number of face-selective clusters in the right hemisphere anatomic ROIs with a threshold of $Z > 3.719$ ($P < 0.0001$) (e.g., 2 individuals have 4 ATL clusters, 1 has 3 clusters, 6 have 2 clusters, etc.). (B) Number of face-selective clusters in the right hemisphere anatomical ROIs for the top voxels (with the highest face-selective SNR), using a fixed volume of 1000 mm³ for all individuals.

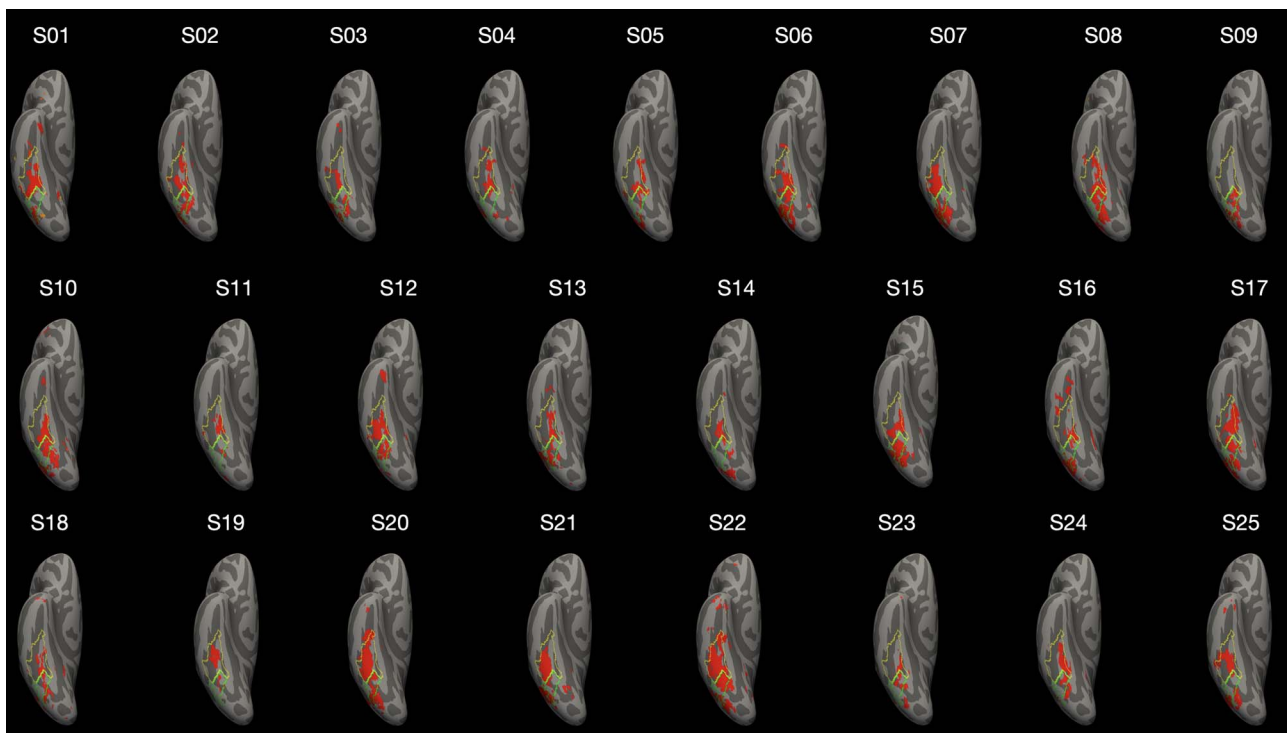


Figure 7. Face-selective activation ($Z > 3.719$, $P < 0.0001$) in the ventral occipitotemporal cortex of the right hemisphere mapped onto a standard cortical surface. The boundaries of cytoarchitectonic areas FG2 (green) and FG4 (yellow) (Rosenke et al. 2017) are outlined.

the individual brains to a standard template (MNI152) and then converted them into Talairach space. Figure 8 shows the distribution of face-selective voxels along the anterior/posterior axis in the VOTC, covering the range between the middle fusiform gyrus and the temporal pole. Even after normalization, variations in anatomical localization are large across individuals. For example, the location of the posterior end of the hippocampus (the red lines in Fig. 8), which is used as the boundary to define the anterior and posterior sections of the temporal lobe, varies substantially in the right hemisphere ($SD = 7.5$ mm).

The distribution of face selective voxels along the posterior/anterior axis in the ventral temporal lobe varies substantially across individuals. In some cases, there is only one peak of the voxel distribution (e.g., S01, S03, S12, S19). In other cases, there are multiple peaks (e.g., S06, S20, S22) (Fig. 8). This variability seems difficult to reconcile with the view that localization of face-selective clusters along the posterior/anterior axis in the VOTC is tightly bonded to cytoarchitectonic areas, as advocated by Grill-Spector and colleagues (see Grill-Spector et al. 2017).

Specifically, these authors suggest that two cytoarchitectonically defined areas in the fusiform gyrus, FG2 and FG4, serve as anatomical constraints for differentiating two different, presumably functionally distinct, face-selective clusters (pFus-faces and mFus-faces in their studies, respectively; see Grill-Spector et al. 2017). To evaluate the validity of this proposed anatomical border with our dataset of multiple clusters, we quantitatively tested whether FG2/FG4 derived from

a standard template can provide less overlap between different face-selective clusters than an arbitrarily defined boundary along the posterior/anterior axis on the fusiform gyrus. As shown in Figure 9, we calculated an overlap index between the two anatomical ROIs and face-selective clusters. If each face-selective cluster lies fully within the boundary of anatomically defined ROIs, then the overlap index would be zero. If all face-selective clusters span across both anatomically defined ROIs, then the overlap index would be 1. Any partial overlap condition would result in an overlap index between 0 and 1 as indicated in Figure 9B. We calculated the overlap index between standard template-based FG2/FG4 or FG3/FG4 ROIs (Rosenke et al. 2017) and our face-selective clusters in the ventral temporal cortex, and compared it to a control condition with five arbitrarily defined anatomical ROIs along the VOTC (Fig. 9C). To do that, we selected five locations (lines) along the posterior/anterior axis as the boundary that arbitrarily separates the fusiform gyrus to a posterior ROI and an anterior ROI. The posterior ROI has the same span as FG2 along the posterior/anterior axis, while the anterior ROI has the same span as FG4 along the posterior/anterior axis.

In both hemispheres, we found an overlap index of around 0.5 in the control condition. While the FG3/FG4 borders separate face-selective clusters better (i.e., lower overlap index) than the control condition, especially in the left hemisphere, the FG2/FG4 borders in both hemispheres were even worse than the control condition in separating face-selective clusters in the fusiform gyrus (Fig. 9D).

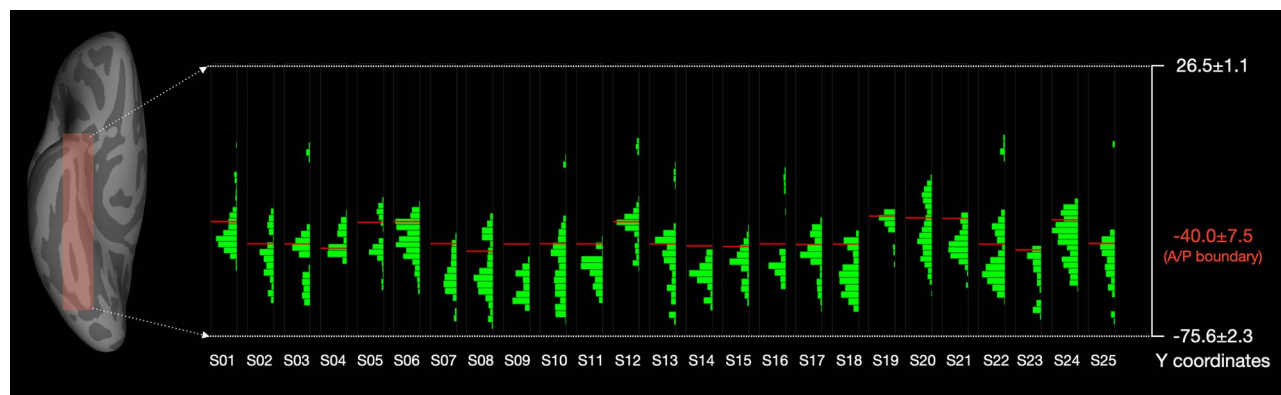


Figure 8. Distribution of face-selective voxels in the right ventral temporal lobe along the posterior/anterior axis (Y). The green bars represent the number of voxels at each of a 3-mm step along the anterior/posterior axis (Y). The red lines mark the location of the posterior end of the hippocampus, which is used as the boundary separating posterior and anterior portions of the temporal lobe (Kim et al. 2000). See Supplementary Figure 4 for the left hemisphere.

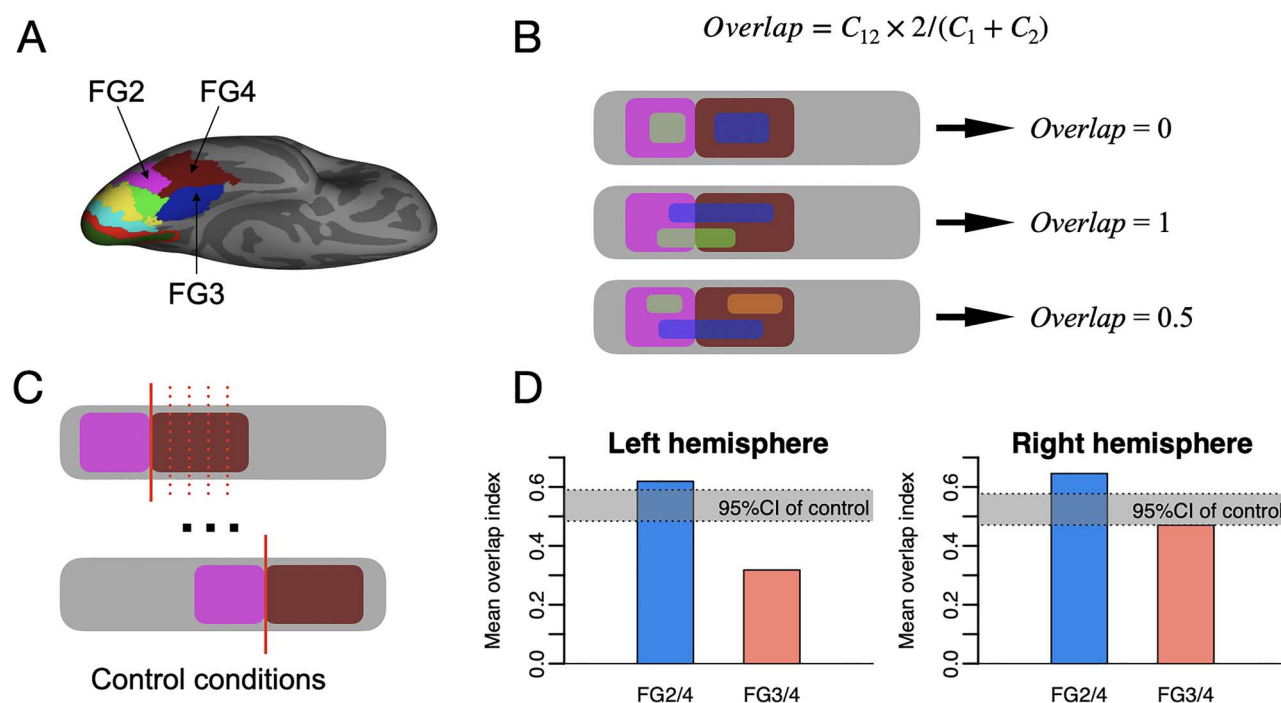


Figure 9. Overlap index between cytoarchitectonic ROIs and face-selective clusters. (A) Standard template of cytoarchitectonic ROIs including FG2 (purple), FG3 (blue), and FG4 (brown). (B) Definition and demonstration of overlap index. The purple and brown areas represent two anatomical ROIs. The areas with other colors represent face-selective clusters. C_{12} represents the number of clusters that overlap with both ROI1 and ROI2. C_1 and C_2 represent the number of clusters that overlap with ROI1 and ROI2, respectively. (C) Arbitrarily defined ROIs. We selected five locations (lines) on the ventral temporal lobe as the boundary between two arbitrarily defined ROIs. The ROI posterior to the boundary (purple) has the same span on the posterior/anterior axis as the FG2, while the ROI anterior to the boundary (brown) has the same span on the posterior/anterior axis as the FG4. (D) Comparison of mean overlap index between cytoarchitectonic ROIs and arbitrarily defined ROIs (see main text).

The same observations were made when using a different procedure, following a reviewer's commentary. Instead of binarizing, we introduced a tolerance level of 80% to represent the "majority of voxels"; that is, if over 80% of voxels fall within one ROI, then it is scored as 0 (no overlap). With this tolerance level, the overall overlap index dropped. However, the pattern remained largely the same: if anything, face-selective clusters are still more likely to cross the FG2/4 boundary than crossing an arbitrary boundary anterior to the FG2/4 boundary (Supplementary Fig. 6).

These results suggest that face-selective clusters in the VOTC are not organized according to a standard

cytoarchitectonic FG2/FG4 border and thus cannot be defined a priori based on such a border.

Interindividual Variability in Face-Selective Clusters Is Independent of Limb-Selective Activation

Given that our fMRI face localizer is based on natural images of faces (and objects), some of these stimuli display limited body cues beyond the face such as the upper torso or shoulders (Fig. 1; see also examples of stimuli and videos in, e.g., Quek and Rossion 2017; Gao et al. 2018; Retter et al. 2020). More generally, the face being a body part, an fMRI face localizer alone does not

exclude voxels that would be recruited to body parts in general without any additional increase in signal to faces specifically. Thus, it could be argued that our localizer with natural images overestimates the number of face-selective voxels, and the number of clusters, in a given individual brain, in particular with respect to regions of the brain that respond selectively to body parts or limbs (Downing et al. 2001; Peelen and Downing 2007; Pinsk et al. 2009; Schwarzlose et al. 2008; Orlov et al. 2010; Weiner and Grill-Spector 2012). While there is no reason to think that this factor would result in an artificial increase rather than a decrease in interindividual “variability” of face-selective clusters, we addressed this issue by testing 4 additional individuals with a new version of our face localizer paradigm in which faces do not include other body parts, as well as with a “limb-localizer” based on the same stimulation principles and parameters (see [Supplementary Methods](#)).

In these four individuals’ brains, we find the typical face-selective clusters, with a large degree of variability in size, location, and number of face-selective clusters, as described in our main experiment ([Fig. 10](#)). Our limb localizer identifies clusters of voxels in typical regions as described in previous studies with a more standard approach, namely in the OTS, the inferior temporal gyrus (ITG) and the middle temporal gyrus (MTG) (Weiner and Grill-Spector 2010). The percentage of overlap between the face-selective and limb-selective voxels is minimal overall (average 27%, range 10–37% for the four subjects or eight hemispheres). Consequently, and most importantly, removing all significant limb-selective voxels (i.e., even those that are less significantly activated for limbs than faces), has little effect on the pattern of face-selective activation and does not affect the number of face-selective clusters in those individuals. For three (participants 1, 2, and 4) out of four individuals, removing overlapping limb-selective voxels from the face-selective voxels did not change the number or spatial distribution of the face-selective clusters. Only in one individual (participant 3), removing limb-selective voxels affected face-selective clusters in the lateral occipital area, but not in the fusiform gyrus.

Discussion

Using a recently developed fMRI face localizer providing high category-selectivity, sensitivity, and test-retest reliability (Gao et al. 2018), we report here a considerable amount of interindividual variability in anatomical localization, spatial extent and number of face-selective clusters in both the human VOTC and STS of 25 individual brains. Below, we first discuss these findings in terms of individual variability in anatomical localization of these clusters, even though this variability has been already addressed and emphasized previously with a different approach (Zhen et al. 2015) and is obviously linked to variations in spatial extent and number of the face-selective clusters. Then, we summarize and discuss

the interindividual variability in terms of the number of face-selective clusters, arguing that this variability is genuine, and finally draw the implications of our observations for understanding the neural basis of human face recognition.

Interindividual Consistency and Variability in Anatomical Localization of Face-Selective Clusters

It is important to state, at the outset, that the large variability in anatomical localization of face-selective clusters across individual brains does not contradict the anatomical consistency of these clusters, as particularly emphasized by Weiner, Grill-Spector, and their colleagues in recent years (Weiner and Grill-Spector 2010, 2012; Lorenz et al. 2017; Weiner et al. 2017; Margalit et al. 2020; Rosenke et al. 2021). Indeed, focusing on posterior brain regions, the vast majority of face-selective clusters across individuals are nested along the VOTC and STS ([Fig. 3](#)). Moreover, within these large-scale regions, face-selective clusters are found on the same cortical gyri and sulci across participants, most significantly in the VOTC, where they are disclosed on the lateral rather than the medial section of the fusiform gyrus ([Fig. 3](#)). These anatomical localizations are entirely consistent with previous fMRI face-localizer studies (e.g., Kanwisher et al. 1997; Fox et al. 2009; Weiner and Grill-Spector 2010; Rossion et al. 2012; Zhen et al. 2015; Gao et al. 2018; Schwarz et al. 2019; Rosenke et al. 2021; see also Jonas et al. 2016; Hagen et al. 2020 for human intracerebral recording evidence in the VOTC).

However, beyond these general organization principles, the large amount of interindividual variability in anatomical localization/spatial distribution of face-selective clusters, particularly in the posteroanterior axis (emphasized here) ([Figs 4, 7, and 8](#)), is also striking. In the ROI defined anatomically as midFus here, in the right hemisphere, even when considering only the 9 individuals out of 25 in which two clusters/maxima are identified (i.e., S02, S03, S05, S07, S09, S10, S12, S22, S24; [Fig. 5](#)), there is considerable anatomical variability in the localization of these clusters with respect to posterior/anterior boundaries defined on an individual basis as the posterior tip of the hippocampus ([Fig. 8](#)). Notably, contrary to previous evidence (Lorenz et al. 2017; Weiner et al. 2017; Rosenke et al. 2021), but in line with the large-scale study of Zhen et al. (2015), we were unable to define just one mFus-faces and one pFus-faces cluster in the right fusiform gyrus in 24 out of 25 participants (18 out of 25 in the left hemisphere). Furthermore, the group-defined anatomical border between FG2 and FG4 is not a good predictor of the localization of the clusters ([Fig. 9](#)).

In this respect, we acknowledge that the real cytoarchitectonic individual borders between FG2 and FG4 could possibly neatly separate two face-selective clusters in our sample. However, such anatomical borders cannot yet be defined in vivo, and we used the same probabilistic

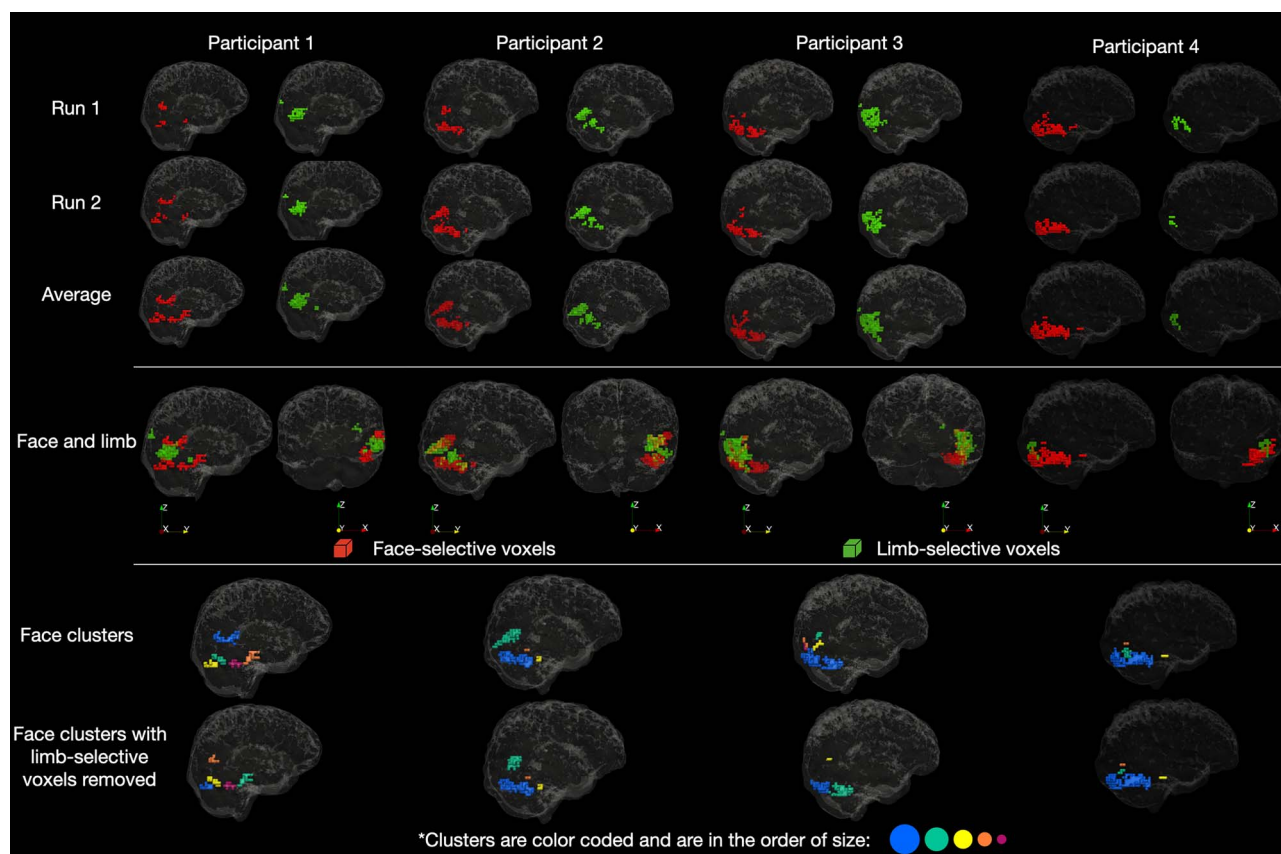


Figure 10. A comparison of face- and limb-selective areas in four individuals within the right lateral occipital and fusiform ROIs. Upper panel: Face- and limb-selective voxels in each run (2 runs) and in the averaged run. Middle panel: Face- and limb-selective voxels (averaged run) overlaid with each other. Bottom panel: Face selective clusters without and with limb-selective voxels removed.

atlas-based approach as in previous studies emphasizing this distinction (Lorenz et al. 2017; Weiner et al. 2017; Schwarz et al. 2019). Moreover, when considering FG2 and FG4 altogether here, most individuals (68% for the right hemisphere) have fewer or more than 2 face-selective clusters/maxima. The anatomical variability of the face-selective clusters is also considerable in the other ROIs considered in the present study, that is, the STS and ATL, even though, due to the use of static visual stimuli here and the drop in SNR due to magnetic susceptibility artifacts, the number of clusters is certainly underestimated in these two latter brain regions.

Overall, our conclusions regarding interindividual variability in localization of face-selective clusters are in line with those of the large-scale study of Zhen et al. (2015). Importantly, we reach these conclusions here with a quite different approach: while Zhen et al. (2015) used a dynamic localizer emphasizing face-selective clusters in the STS, instead, we used an fMRI localizer in which static natural images are presented at a fast periodic stimulation rate (Gao et al. 2018, 2019), inspired from validated frequency-tagging studies in electroencephalography (EEG; e.g., Rossion et al. 2015; Quok and Rossion 2017). Compared with the study of Zhen et al. (2015), our approach may result in a reduced face-selective response in the STS, in particular in its middle and anterior sections (Fig. 3), but

conveys substantial advantages in terms of sensitivity, specificity and reliability. In particular, thanks to the use of highly variable natural images rather than stimulus sets maximizing within-category homogeneity and systematic shape differences between categories, the present approach is optimal to exclude spurious “face-selective” responses in low-level visual areas (Gao et al. 2018). Moreover, compared with this previous study, no spatial smoothing was applied here.

As Zhen et al. (2015) put it, interindividual variability in anatomical localization of the face-selective clusters is not surprising given the considerable amount of variability in size and location of cytoarchitectonic (visual) areas across individuals (e.g., Amunts et al. 1999; Malikovic et al. 2007; Rottschy et al. 2007; Fischl et al. 2008; Caspers et al. 2013; Lorenz et al. 2017) as well as interindividual variability in anatomical connectivity (Bürgel et al. 2006; Vassal et al. 2018; Bernard et al. 2019). On top of that, different face recognition functions, in particular face identity recognition, undergo a long developmental course in the human species (Carey 1992; Hills and Lewis 2018) and individual adults can vary substantially in face identity recognition performance (e.g., Bowles et al. 2009; McCaffery et al. 2018). Therefore, variability in size, height and localization of face-selective clusters is certainly increased by the various quantitative and qualitative experiences in face recognition of different

individual observers, even in a relatively highly homogeneous population (i.e., all young adults, 84% of Caucasian origin, right-handed). It is also likely that anatomicofunctional connectivity between these clusters varies substantially across individuals (Bürge et al. 2006; Mueller et al. 2013; Chamberland et al. 2017; although see Wang et al. 2020).

Interindividual Variability in Number of Face-Selective Clusters

The large degree of interindividual variability in size, height and spatial extent of face-selective clusters has long been known, and can in fact be appreciated in any fMRI study reporting individual data of a given face localizer. However, despite hinting at such variability in a previous large-scale study (Rossion et al. 2012; see also Schwarz et al. 2019), to our knowledge, no fMRI study has systematically described and emphasized interindividual variability in the number of face-selective clusters. In the aforementioned study of Zhen et al. (2015), 6 labeled clusters were a priori defined to be identified in all individual brains, using interjudges' agreement to identify these clusters in different anatomical regions. A number of clusters were reported as "missing", and the number of unlabeled clusters in individual brains were not reported. Moreover, the substantial spatial smoothing (i.e., Gaussian filter of 6-mm FWHM) applied to the data in that study probably merged local maxima and clusters together (see Supplementary Fig. 5).

In contrast, in the present study, without applying any spatial smoothing, but nevertheless using conservative criteria in terms of statistical significance, size (minimum of 81 mm³, corresponding to about 2.5 million of neurons according to neuronal density estimates in the fusiform gyrus; Chance et al. 2013) and reliability to identify clusters, the variability in number of clusters could freely "emerge" from the data. This approach leads to an impressive amount of interindividual variability in the number of face-selective clusters, particularly in the VOTC (including the ATL), where we find between 1 and 7 clusters across our 25 individuals tested (Fig. 5), but also in the pSTS, where the number of face-selective clusters varies between 0 and 4 (Fig. 6). Moreover, in many face-selective clusters, several local maxima can be identified and could easily constitute clusters of their own if more severe statistical thresholds were used (Fig. 5; see also Supplementary Fig. 3).

It is legitimate to wonder whether the interindividual variability described here is genuine, or simply due to (variability in) measurement and analysis procedures (i.e., noise) of the present study. In terms of measurement, here all participants were tested in the same conditions, with the same stimulation protocol. Although the stimulation paradigm used is unconventional, it has been previously validated, showing for instance the highest average z-score at the group level in the right hemispheric lateral middle fusiform gyrus at virtually identical locations as in previous studies (e.g., 42, -54,

-14 in Talairach coordinates here, for 40, -55, -10 in Kanwisher et al. 1997 with a block design localizer; 42, -51, -14 in Zhen et al. 2015 with a dynamic localizer) and an extremely high spatial overlap ($91\% \pm 8\%$) in the Fusiform Gyrus with a conventional (block design) mode of stimulation using the same—balanced number—of face and nonface object stimuli (Gao et al. 2018). Moreover, the surface maps presented here are very similar to surface maps shown in other studies (e.g., Figs 3 and 7 here vs. Fig. 4 in Weiner and Grill-Spector 2010).

As the present frequency-tagging face localizer has increased sensitivity (i.e., SNR), one could argue that this is a key factor leading to an increase in number and interindividual variability in the VOTC and STS compared with other face localizers. However, contrary to standard stimulation modes and localizers performed with more homogenous stimulus sets for both faces and the compared object stimuli (e.g., Rice et al. 2014), the paradigm used here eliminates the contributions of low-level visual cues contained in the image amplitude spectrum (Gao et al. 2018), which could have artificially increased interindividual variability in the number of significant clusters. Moreover, despite its high sensitivity and internal reliability (see Gao et al. 2018), if anything, due to the use of static images and the inevitable drop of SNR in the ATL particularly with conventional fMRI sequences (Wandell 2011; Axelrod and Yovel 2013; Rossion et al. 2018; Fig. 3), the present study rather certainly underestimates the number and degree of interindividual variability in face-selective clusters, in particular in the STS and in the anterior portions of the VOTC.

An issue worth considering is the relatively high rate of visual stimulation in our paradigm, with a stimulus onset asynchrony of only 166 ms between each face and a nonface object stimulus (Fig. 1). EEG frequency-tagging studies with this paradigm have shown comparable amplitude and interindividual variability of face-selective activity at 6 Hz and much slower rates (i.e., 3 Hz), and no decrease in amplitude with increasing rates to 12 Hz, and little decrease up to 20 Hz (Retter et al. 2020), indicating that a 6 Hz rate is not too fast to elicit a full face-selective response in every individual. Moreover, the alternation between a face and nonface stimulus within a "mini-burst" (Fig. 1) does not only minimize category-based adaptation effects (as in conventional fMRI block designs) but provides an SOA of 333 ms between two face stimuli, allowing to capture the bulk of the neural face-selective response elicited by each stimulus (Retter and Rossion 2016), these two factors contributing to the very high SNR observed with this paradigm (Gao et al. 2018). Finally, a 6-Hz stimulation rate is also largely sufficient to even individuate each presented face (Retter et al. 2021), and ensures that there is only a single glance at each face stimulus, reducing differential eye movements between individual subjects that could artificially increase interindividual variability.

A more important issue is the type of comparison that is performed, that is, faces versus all types of living and nonliving object categories mixed up together to identify face-selective clusters. We argue that this factor is unlikely to play a significant role in artificially generating interindividual variability in localization and number of face-selective clusters, for several reasons. First, a large number of face localizers in fMRI rely on this type of comparison (Berman et al. 2010) (albeit with segmented items and less variable images, limiting generalization) and nevertheless describe/report only a few well-defined face-selective clusters (OFA, FFA, pSTS usually) (e.g., Rossion et al. 2003; Grill-Spector et al. 2004; Caldara et al. 2006; Schiltz and Rossion 2006). Second, there is no evidence that contrasting faces to multiple object categories together artificially inflates face selectivity as compared with face localizers in which exemplars of a single category (e.g., cars or houses; Rossion et al. 2012; Schwarz et al. 2019; Horowitz et al. 2004; Pourtois et al. 2005; Löffler et al. 2005) or a few selected categories (e.g., objects, characters, limbs, places; Weiner et al. 2017) are compared one-by-one to faces (see Berman et al. 2010).

Specifically, according to their organizational framework of category-selectivity in the lateral and ventral occipitotemporal cortex, Weiner, Grill-Spector and colleagues argue that limbs/body parts generate category-selective responses laterally on the occipitotemporal sulcus and in between face-selective clusters in the posteroanterior axis, guiding the definition of (a fixed set of) face-selective regions (Weiner and Grill-Spector 2010, 2012). However, there is no direct evidence that including limbs/body parts as contrast stimuli reduces the number of face-selective clusters in the lateral and ventral occipitotemporal cortex, and our complementary study in 4 individuals shows minimal overlap between face-selective and limb-selective voxels (Fig. 10). More fundamentally, if these OTS-limb regions (or regions of the inferior temporal gyrus) respond significantly more to faces than to all other categories than limbs (Weiner and Grill-Spector 2010), it is difficult to argue that they do not contribute significantly to face categorization. Finally, our complementary study shows that removing the limbs/body parts-selective voxels from our analysis, does not affect our conclusions regarding the number of face-selective clusters and their interindividual variability (Fig. 10). In summary, while we cannot fully exclude that adding many other visual categories to compare one-by-one to faces would lead to a well-structured organization of category-selectivity in the VOTC with only 3 well-defined face-selective clusters (IOG, pFus-faces, and mFus-faces) falling in corresponding anatomical regions in each individual brain, both an objective look at others' data (e.g., Fig. 4 of Weiner and Grill-Spector 2010) and ours makes it very unlikely.

As for the analysis steps, we used a model-free approach, such that variability across individuals and regions cannot be due to variability in the relation between neural activity and a modeled hemodynamic

response (e.g., Buxton et al. 2004; Havlicek et al. 2015). While some participants performed only two and others three runs, this was taken into account in the analysis to use the same statistical threshold across individuals (see [Materials and Methods](#)).

Finally, one could argue that interindividual variability in the number of face-selective clusters as reported here could be merely due to failures in disclosing genuine clusters in some individual brains at a given statistical threshold, or the use of a too liberal statistical threshold, forcing different clusters to merge together. However, not only did we take particular care in using a conservative threshold and describing both the clusters and local maxima, but our conclusions of interindividual variability in number and anatomical localization would remain the same if the threshold changed uniformly across individuals (Fig. 6; see also [Supplementary Fig. 3](#)). Moreover, across individuals, the variability in the number of clusters is not related to the statistical threshold used, or to total face-selective volume activated or maximal SNR. A different strategy would be to set the number of face-selective clusters to be identical across individuals (e.g., 4 in the VOTC) by using variable statistical thresholds (Rossion et al. 2012). Yet, this would lead to clearly identifiable clusters in only a subset of individual brains (i.e., those with a minimum of 4 clusters, e.g., 10 individuals for the right VOTC), and these 4 clusters would then not correspond at all to the same 4 discrete anatomical regions across individuals (Fig. 4).

Overall, these observations therefore support the view that—at least at the standard fMRI resolution used here—interindividual variability in terms of number of face-selective clusters in the human adult brain, spanning across different cortical areas, is not due to noise.

Implications for the Neural Basis of Human Face Recognition

Given that neuroimaging studies of human face recognition have been performed for three decades, one may wonder why interindividual variability in the number of face-selective clusters has not been reported and is barely even mentioned in previous fMRI studies (except in Rossion et al. 2012, but without any quantification and a less specific and sensitive approach). One reason is that few fMRI studies focus on face localizer data, and even fewer on an extensive spatial analysis of such data (Ishai et al. 2005; Weiner and Grill-Spector 2010, 2012; Rossion 2012; Zhen et al. 2015; Schwartz et al. 2019; Wang et al. 2020). Rather, functional fMRI localizers are used—by definition—to localize functional regions that are subsequently tested for experimental effects that are the main focus of the study (Saxe and Powell 2006; Kanwisher 2017). Moreover, these studies often even focus on a single cluster, usually the largest one in the middle fusiform gyrus, defined across individual brains as the FFA with distinct, largely subjective, criteria across studies.

A second reason for neglecting interindividual variability in cluster number is that the vast majority of fMRI studies of human face recognition apply relatively severe (Gaussian) spatial smoothing to their data in order to improve SNR and conform to the assumptions of the Random Field Theory for statistical testing (Worsley 2005). An obvious consequence of such spatial smoothing is that different face-selective clusters are merged together, artificially reducing their number (see Weiner and Grill-Spector 2012; and as also shown in Supplementary Fig. 5). Even if they end up in vastly different locations across individuals, these face-selective clusters are usually subjectively labeled with the same acronym for group analyses and for deriving general conclusions. A third reason is that interindividual variability in number of clusters can easily be dismissed as being due to variations in local SNR in fMRI. On this basis, small clusters are ignored, or nearby clusters are lumped together as being part of the same region, a practice that may be common in fMRI research. Admittedly, fluctuations of the fMRI BOLD signal across individual brains and brain regions can be due to many factors beyond the number, density and intensity of activity of neuronal populations involved (e.g., proximity of veins, magnetic susceptibility artifacts, motion, etc.; Logothetis 2008). Even though a very conservative procedure of selecting voxels that are only reliably activated across several functional runs can be used as here, these factors cannot be fully—or even well—controlled for, and can always be used to justify interindividual variability in the number of disclosed functional clusters.

This leads to the fourth, and most important, reason to dismiss interindividual variability in face-selective cluster numbers: theory. That is, general neurofunctional models have been proposed in the early stages of the neuroimaging investigation of the neural basis of face recognition, constraining the systematic search for “the exact same number” of face-selective clusters—typically defined as regions or areas—in each individual brain (i.e., OFA, FFA, and pSTS in Haxby et al. 2000). When other face-selective clusters are labeled in subsequent studies that become influential (e.g., FFA1 and FFA2 in Pinsk et al. 2009; pFus-faces and mFus-faces, described by Weiner and Grill-Spector 2010; a face-selective cluster in ATL reported by Rajimehr et al. 2009 and a number of other studies, although with substantially different locations across studies), these clusters are added in refined neurofunctional models (Duchaine and Yovel 2015). Such models are nevertheless always built upon the assumption that the number of face-selective regions, and their connections, are the same across individual human brains (and also largely across the primate order; Yovel and Freiwald 2013; Hung et al. 2015; Weiner and Grill-Spector 2015; Hesse and Tsao 2020; but see Rossion and Taubert 2019). The chief reason behind this assumption is not only that scientific research is about generality of principles rather than idiosyncratic features but that the

standard view in cognitive neuroscience implies such uniformity.

That is, according to the prevalent view, visual recognition is thought to be decomposable in discrete representational stages (which are largely thought to be hierarchical, but could also be initiated/performed in cascade or in parallel) with computational transformations applied to these representations (Marr 1982; Grill-Spector and Malach 2004; Di Carlo and Cox 2007; Grill-Spector et al. 2017). This view is largely embraced in both cognitive and neurocognitive models of human face recognition (Bruce and Young 1986; Haxby et al. 2000; Calder and Young 2005; Duchaine and Yovel 2015; see also Freiwald 2020; Hesse and Tsao 2020 in nonhuman primates). Therefore, according to the standard view of the neurofunctional organization of face recognition, all individual brains of neurotypical adults must necessarily hold the same number of discrete face-selective clusters/regions located in the same anatomical areas, while variability in functional localization would be due to noise or to anatomical variations in gyri and variability in the exact position and size of subpopulations of neurons activated within these areas. According to this framework, “counting the number of clusters that are face-selective is not a productive method in determining the computations involved in face perception” (Weiner and Grill-Spector 2010, p. 1570).

If, however, there is interindividual variability in the number of face-selective clusters across variable anatomical areas, this standard view is seriously challenged: how could the same function be performed across individual brains with a variable number of computational/representational stages, and how could these stages be functionally characterized? A full discussion of this issue is, obviously, beyond the scope of the present paper. Nevertheless, it deserves at least a few theoretical and methodological considerations.

At the theoretical level, recognizing faces may be essentially based on the production of a selective (i.e., discriminant) neural response which can be reliably generalized across variable inputs (i.e., “recognition” as a categorization function; Rossion and Retter 2020). Beyond the recognition of a stimulus as a face, all other face recognition functions (e.g., gender, identity, expression, etc.) could be defined and expressed as such. Hence, recognition “only” requires a population of neurons (either local, e.g., a minicolumn, or spatially distributed across different brain regions) to change (through excitation or inhibition, or both) its firing rate selectively (i.e., fire more or actively reduce firing to faces, not to other visual shapes) and reliably (with high consistency for variable presentations of faces). Such a function could be simply achieved by noncategorical sensory inputs from lower order brain areas (i.e., primary visual cortex and other topographical visual areas) triggering the activation of a specialized population of neurons, or a cortical circuit, in higher level brain areas. As this circuit

must be shaped by experience, its populations of neurons have been selected together based on their joined activity during successful recognition of stimuli as faces in the past. Hence, sensory inputs coming from early visual areas trigger a face-selective cortical response not only because of their intrinsic spatiotemporal characteristics but because similar patterns of inputs have led to successful activation of the face-selective circuitry in previous experiences and adaptive behavior. The cortical face-selective neural network, being shaped by variable individual experiences on top of intrinsic anatomical variability determined by genetic factors, therefore increases in variability across individuals.

According to this view, populations of neurons in this circuit cluster (i.e., they form “nodes” in the cortical face network) because of the ecological relevance and dominance of faces in the visual environment coupled with the intrinsic organization of neurons in competing (mini)columns, in which neurons that fire together “wire together” (Hebb 1949; Edelman and Mountcastle 1978; Mountcastle 1997; Feldman 2009; Buxhoeveden 2012). All along development, an initially continuous but coarse (i.e., unspecific) neuronal population response along the lateral VOTC to faces may therefore progressively “break down in pieces” (i.e., form several clusters) through competition with other categories while, in return, increase in specificity in response to faces. Spatially distinct face-selective clusters remain heavily interconnected (Wang et al. 2020) and, as they concentrate a high density of selective populations of neurons, are functionally meaningful, as shown by the striking and specific effects of focal electrical stimulation of these clusters on face perception and face identity recognition (Jonas et al. 2012; Parvizi et al. 2012; see Jonas and Rossion 2021 for review).

Importantly, this is not to say that different populations of neurons in face-selective clusters all along the VOTC have the same response properties, that is, fire to the same inputs. Indeed, depending on their relative position within the network, their intrinsic and extrinsic pattern of connectivity can vary. For instance, anterior/ventral face-selective clusters may receive relatively more foveal inputs than posterior/lateral clusters from early visual cortical areas (Finzi et al. 2021). Moreover, face-selective clusters in posterior brain regions may have direct reentrant connections with early visual (i.e., topographical) areas, while face-selective clusters anterior to the fusiform gyrus may be directly connected with multimodal regions in the ATL and the hippocampus (Jonas and Rossion 2021). Interindividual variability in the number and spatial extent of face-selective clusters is not an issue as long as their functional sensitivities (e.g., peripheral/foveal or visuo/semantic) vary gradually, in particular along the posteroanterior axis of the VOTC, rather in terms of fixed hierarchical information-processing representational “stages.” Focal damage to these clusters, or electrical intracerebral stimulation, can therefore have different behavioral consequences (Jonas

and Rossion 2021), which are nevertheless difficult to account for in terms of a modular organization.

In sum, the human face recognition function is not strictly localized to one anatomical region such as the “FFA” in the lateral middle fusiform gyrus, and not even supported by an anatomically fixed set of discrete regions across individual brains. Yet, it is “not fully distributed” either in the whole VOTC (e.g., Haxby et al. 2001; O’Toole et al. 2005),² but obeys general anatomical constraints to define idiosyncratic cortical networks with a substantial amount of variability in the configuration (i.e., localization, size spatial extent, and number) of their nodes.

This briefly sketched alternative view of the neuro-functional organization of face recognition also carries a number of methodological implications for future studies and understanding of the neural basis of human face recognition with fMRI and neuroimaging approaches in general. One implication is that while using face-selective clusters to ask questions about category-specific mechanisms of, say, attention or consciousness, appears to be valid and informative, attempts to relate face-selective clusters one by-one across individual brains to define “the” function (representation/computation) of each cluster (e.g., “the” FFA) are unlikely to succeed. Even more so, searching for one-to-one homologies or comparisons of face-selective clusters between humans and other primates (Tsao et al. 2008; Yovel and Freiwald 2013; Weiner and Grill-Spector 2015) appears profoundly misleading. While some fMRI studies appear to constantly report six face-selective clusters in posterior regions of the macaque brain for instance (Tsao et al. 2008), with four to five of these clusters located in the STS, this exact number is rarely reported in most studies, with variations between 2 and 6 clusters or more (Pinsk et al. 2005, 2009; Hadj-Bouziane et al. 2008; Moeller et al. 2008; Tsao et al. 2008; Taubert et al. 2015, 2020), suggesting also a large amount of interindividual variability in this nonhuman primate species. In humans, using probabilistic atlases based on independent datasets to define face-selective regions in an individual brain based on cortical anatomy only (e.g., Rosenke et al. 2021) is also questionable at two levels: first because this approach will lead to a poor evaluation of face selectivity in the studied brain (Fig. 7), and second because, by lumping together all clusters selective to one domain in a given cytoarchitectonic area, it reinforces a misleading vision of the brain as being constituted of the same number of functional modules, further ignoring interindividual functional variability.

Evaluating what type of stimulus properties or task-factors modulates neural activity in the face-selective

² This view of a widely distributed face representation is based on the observation that there is sufficient “information” [i.e., patterns of variations of signal across voxels] for faces to be reliably recognized/categorized even when removing the contribution of face-selective regions [Haxby et al. 2001]. However, there is no evidence that this category recognition outside of face-selective regions is reliable beyond simple image-based matching of few contrasted exemplars, and useful for the function at stake.

network is legitimate, but this analysis should be preferably considered at the level of the whole cortical face network, testing for gradients of functional responses to physical or abstract properties in different axes, rather than focusing on necessarily subjectively defined functional regions. Searching for specific patterns of anatomico-functional connectivity that can be generalized across individual brains, for example, FFA connected to OFA, and so on (e.g., Wang et al. 2020; Kessler et al. 2021), also appears problematic insofar as the definition of specific isolated clusters is not clear. However, studies of anatomico-functional connectivity of the cortical face network can be highly relevant at level of individual brains.

The same issue also applies to transcranial magnetic stimulation (TMS) studies, where average coordinates are sometimes used to define target stimulation sites for face recognition (e.g., Pitcher et al. 2007). In fact, the data illustrated here show that in many individuals, face-selective clusters expand considerably, continuously, across anatomical borders (Figs 7 and 9). This apparent continuity may—or may not be—broken with higher-resolution data obtained at high field fMRI, which should be the topic of future research. Regardless, this field of study would be well inspired by abandoning functional labels such as “FFA” or “OFA” because they only correspond to a seriously distorted, and therefore misleading reality (Rossion et al. 2012). Rather, face-selective clusters may be better referred to “at the individual level” in terms of their predominant anatomical location (“Fus-faces 1,” “Fus-faces 2”), fully acknowledging that they can extend over different anatomical structures and do not necessarily correspond across individual brains.

Supplementary Material

Supplementary material can be found at *Cerebral Cortex* online.

Notes

We thank three anonymous reviewers for their careful evaluation and constructive comments on a previous version of this manuscript. *Conflict of Interest*: The authors declared no conflict of interest.

Funding

Excellence of Science (EOS) program (HUMVISCAT-30991544) to B.R.; Fundamental Research Funds for the Central Universities of China (2019QN81013) to X.G.; Zhejiang University Global Partnership Fund (188170-11103) to X.G.; Zhejiang University Startup Fund to X.G.

References

- Allison T, Puce A, McCarthy G. 2000. Social perception from visual cues: role of the STS region. *Trends Cogn Sci*. 4(7):267–278. [https://doi.org/10.1016/S1364-6613\(00\)01501-1](https://doi.org/10.1016/S1364-6613(00)01501-1).
- Amunts K, Schleicher A, Bürgel U, Mohlberg H, Uylings HBM, Zilles K. 1999. Broca's region revisited: cytoarchitecture and intersubject variability. *J Comp Neurol*. 412(2). [https://doi.org/10.1002/\(SICI\)1096-9861\(19990920\)412:2<319::AID-CNE10>3.0.CO;2-7](https://doi.org/10.1002/(SICI)1096-9861(19990920)412:2<319::AID-CNE10>3.0.CO;2-7).
- Andrews TJ, Schluppeck D, Homfray D, Matthews P, Blakemore C. 2002. Activity in the fusiform gyrus predicts conscious perception of Rubin's vase-face illusion. *Neuro Image*. 17(2):890–901. <https://doi.org/10.1006/nimg.2002.1243>.
- Axelrod V, Yovel G. 2013. The challenge of localizing the anterior temporal face area: a possible solution. *Neuro Image*. 81:371–380. <https://doi.org/10.1016/j.neuroimage.2013.05.015>.
- Berman MG, Park J, Gonzalez R, Polk TA, Gehrke A, Knaffla S, Jonides J. 2010. Evaluating functional localizers: the case of the FFA. *Neuro Image*. 50(1):56–71. <https://doi.org/10.1016/j.neuroimage.2009.12.024>.
- Bernard F, Zemmoura I, Ter Minassian A, Lemée JM, Menei P. 2019. Anatomical variability of the arcuate fasciculus: a systematic review. In: *Surgical and radiologic anatomy* (vol. 41, Issue 8). <https://doi.org/10.1007/s00276-019-02244-5>.
- Bernstein M, Yovel G. 2015. Two neural pathways of face processing: a critical evaluation of current models. *Neurosci Biobehav Rev*. 55: 536–546. <https://doi.org/10.1016/j.neubiorev.2015.06.010>.
- Bowles DC, McKone E, Dawel A, Duchaine B, Palermo R, Schmalzl L, Rivolta D, Wilson CE, Yovel G. 2009. Diagnosing prosopagnosia: effects of ageing, sex, and participant-stimulus ethnic match on the Cambridge face memory test and Cambridge face perception test. *Cogn Neuropsychol*. 26(5):423–455. <https://doi.org/10.1080/02643290903343149>.
- Bruce V, Young A. 1986. Understanding face recognition. *Br J Psychol*. 77(3):305–327.
- Bürgel U, Amunts K, Hoemke L, Mohlberg H, Gilsbach JM, Zilles K. 2006. White matter fiber tracts of the human brain: three-dimensional mapping at microscopic resolution, topography and intersubject variability. *Neuro Image*. 29(4):1092–1105. <https://doi.org/10.1016/j.neuroimage.2005.08.040>.
- Buxhoeveden DP. (2012). Minicolumn size and human cortex. In *Progress in brain research* (vol. 195). <https://doi.org/10.1016/B978-0-444-53860-4.00010-6>.
- Buxton RB, Uludağ K, Dubowitz DJ, Liu TT. 2004. Modeling the hemodynamic response to brain activation. *Neuro Image*. 23 (suppl. 1): S220–S233. <https://doi.org/10.1016/j.neuroimage.2004.07.013>.
- Caldara R, Seghier ML, Rossion B, Lazeyras F, Michel C, Hauert CA. 2006. The fusiform face area is tuned for curvilinear patterns with more high-contrasted elements in the upper part. *Neuro Image*. 31: 313–319. <https://doi.org/10.1038/nrn1724>.
- Calder AJ, Young AW. 2005. Understanding the recognition of facial identity and facial expression. *Nat Rev Neurosci*. 6(8):641–651. <https://doi.org/10.1038/nrn1724>.
- Carey S. 1992. *Becoming a Face Expert*. 335(1273):95–102. <https://doi.org/10.1098/rstb.1992.0012>.
- Caspers S, Schleicher A, Bacha-Trams M, Palomero-Gallagher N, Amunts K, Zilles K. 2013. Organization of the human inferior parietal lobule based on receptor architectonics. *Cereb Cortex*. 23(3):615–628. <https://doi.org/10.1093/cercor/bhs048>.
- Chamberland M, Girard G, Bernier M, Fortin D, Descoteaux M, Whittingstall K. 2017. On the origin of individual functional connectivity variability: the role of white matter architecture. *Brain Connect*. 7(8):491–503. <https://doi.org/10.1089/brain.2017.0539>.
- Chance SA, Sawyer EK, Clover LM, Wicinski B, Hof PR, Crow TJ. 2013. Hemispheric asymmetry in the fusiform gyrus distinguishes Homo sapiens from chimpanzees. *Brain Struct*.

- Funct. 218(6):1391–1405. <https://doi.org/10.1007/s00429-012-0464-8>.
- Destrieux C, Fischl B, Dale A, Halgren E. 2010. Automatic parcellation of human cortical gyri and sulci using standard anatomical nomenclature. *Neuro Image*. 53(1):1–15. <https://doi.org/10.1016/j.neuroimage.2010.06.010>.
- Downing PE, Jiang Y, Shuman M, Kanwisher N. 2001. A Cortical Area Selective for Visual Processing of the Human Body. *Science*. 293:2470–2473.
- Duchaine B, Yovel G. 2015. A revised neural framework for face processing. *Annu Rev Vis Sci*. 1(1):393–416. <https://doi.org/10.1146/annurev-vision-082114-035518>.
- Duncan KJ, Pattamadilok C, Knierim I, Devlin JT. 2009. Consistency and variability in functional localisers. *Neuro Image*. 46:1018–1026.
- Edelman GM, Mountcastle VB. 1978. *The mindful brain: cortical organization and the group-selective theory of higher brain function*. Cambridge, MA: MIT Press.
- Elbich DB, Scherf KS. 2017. Beyond the FFA: brain-behavior correspondences in face recognition abilities. *Neuro Image*. 147:409–422. <https://doi.org/10.1016/j.neuroimage.2016.12.042>.
- Elbich DB, Molenaar PCM, Scherf KS. 2019. Evaluating the organizational structure and specificity of network topology within the face processing system. *Hum Brain Mapp*. 40(9):2581–2595. <https://doi.org/10.1002/hbm.24546>.
- Engel AD, McCarthy G. 2013. Probabilistic atlases for face and biological motion perception: an analysis of their reliability and overlap. *Neuro Image*. 74:140–151. <https://doi.org/10.1016/j.neuroimage.2013.02.025>.
- Fairhall SL, Ishai A. 2007. Effective connectivity within the distributed cortical network for face perception. *Cereb Cortex*. 17(10):2400–2406. <https://doi.org/10.1093/cercor/bhl148>.
- Fang F, He S. 2005. Viewer-centered object representation in the human visual system revealed by viewpoint aftereffects. *Neuron*. 45(5):793–800. <https://doi.org/10.1016/j.neuron.2005.01.037>.
- Feldman DE. 2009. Synaptic mechanisms for plasticity in neocortex. in. *Annu Rev Neurosci*. 32:33–55. <https://doi.org/10.1146/annurev.neuro.051508.135516>.
- Fenzi D, Gomez J, Nordt M, Rezai AA, Poltoratski S, Grill-Spector K. 2021. Differential spatial computations in ventral and lateral face-selective regions are scaffolded by structural connections. *Nat Commun*. 12(1):2278. <https://doi.org/10.1038/s41467-021-22524-2>.
- Fischl B, Rajendran N, Busa E, Augustinack J, Hinds O, Yeo BTT, Mohlberg H, Amunts K, Zilles K. 2008. Cortical folding patterns and predicting cytoarchitecture. *Cereb Cortex*. 18(8):1973–1980. <https://doi.org/10.1093/cercor/bhm225>.
- Frässle S, Paulus FM, Krach S, Jansen A. 2016. Test-retest reliability of effective connectivity in the face perception network. *Hum Brain Mapp*. 37:730–744.
- Fox CJ, Iaria G, Barton JJS. 2009. Defining the face processing network: optimization of the functional localizer in fMRI. *Hum Brain Mapp*. 30(5):1637–1651. <https://doi.org/10.1002/hbm.20630>.
- Freiwald WA. 2020. Social interaction networks in the primate brain. *Curr Opin Neurobiol*. 65:49–58. <https://doi.org/10.1016/j.conb.2020.08.012>.
- Gao X, Gentile F, Rossion B. 2018. Fast periodic stimulation (FPS): a highly effective approach in fMRI brain mapping. *Brain Struct Funct*. 223(5):2433–2454. <https://doi.org/10.1007/s00429-018-1630-4>.
- Gao X, Vuong QC, Rossion B. 2019. The cortical face network of the prosopagnosic patient PS with fast periodic stimulation in fMRI. *Cortex*. 119:528–542. <https://doi.org/10.1016/j.cortex.2018.11.008>.
- Gauthier I, Tarr MJ, Moylan J, Skudlarski P, Gore JC, Anderson AW. 2000. The fusiform “face area” is part of a network that processes faces at the individual level. *J Cogn Neurosci*. 12(3):495–504. <http://www.ncbi.nlm.nih.gov/pubmed/10931774>.
- Gauthier I, Curby KM, Skudlarski P, Epstein RA. 2005. Individual differences in FFA activity suggest independent processing at different spatial scales. *Cogn Affect Behav Neurosci*. 5(2):222–234. <https://doi.org/10.3758/CABN.5.2.222>.
- Golarai G, Ghahremani DG, Whitfield-Gabrieli S, Reiss A, Eberhardt JL, Gabrieli JDE, Grill-Spector K. 2007. Differential development of high-level visual cortex correlates with category-specific recognition memory. *Nat Neurosci*. 10(4):512–522. <https://doi.org/10.1038/nn1865>.
- Golarai G, Liberman A, Grill-Spector K. 2015. Experience shapes the development of neural substrates of face processing in human ventral temporal cortex. *Cereb Cortex*. 27(2):bhv314. <https://doi.org/10.1093/cercor/bhv314>.
- Grill-Spector K, Malach R. 2004. The human visual cortex. *Annu Rev Neurosci*. 27(1):649–677. <https://doi.org/10.1146/annurev.neuro.27.070203.144220>.
- Grill-Spector K, Knouf N, Kanwisher N. 2004. The fusiform face area subserves face perception, not generic within-category identification. *Nat Neurosci*. 7(5):555–562. <https://doi.org/10.1038/nn1224>.
- Grill-Spector K, Weiner KS, Kay K, Gomez J. 2017. The functional neuroanatomy of human face perception. *Annu Rev Vis Sci*. 3(1):167–196. <https://doi.org/10.1146/annurev-vision-102016-061214>.
- Gschwind M, Pourtois G, Schwartz S, Van De Ville D, Vuilleumier P. 2012. White-matter connectivity between face-responsive regions in the human brain. *Cereb Cortex*. 22(7):1564–1576. <https://doi.org/10.1093/cercor/bhr226>.
- Hadj-Bouziane F, Bell AH, Knusten TA, Ungerleider LG, Tootell RBH. 2008. Perception of emotional expressions is independent of face selectivity in monkey inferior temporal cortex. *Proc Natl Acad Sci U S A*. 105(14):5591–5596. <https://doi.org/10.1073/pnas.0800489105>.
- Hagen S, Jacques C, Maillard L, Colnat-Coulbois S, Rossion B, Jonas J. 2020. Spatially dissociated intracerebral maps for face- and house-selective activity in the human ventral Occipito-temporal cortex. *Cereb Cortex*. 30(7):4026–4043. <https://doi.org/10.1093/cercor/bhaa022>.
- Halgren E, Dale AM, Sereno MI, Tootell RBH, Marinkovic K, Rosen BR. 1999. Location of human face-selective cortex with respect to retinotopic areas. *Hum Brain Mapp*. 7(1):29–37. [https://doi.org/10.1002/\(SICI\)1097-0193\(1999\)7:1<29::AID-HBM3>3.0.CO;2-R](https://doi.org/10.1002/(SICI)1097-0193(1999)7:1<29::AID-HBM3>3.0.CO;2-R).
- Havlicek M, Roebroeck A, Friston K, Gardumi A, Ivanov D, Uludag K. 2015. Physiologically informed dynamic causal modeling of fMRI data. *Neuro Image*. 122:355–372. <https://doi.org/10.1016/j.neuroimage.2015.07.078> <http://www.ncbi.nlm.nih.gov/pubmed/10827445>.
- Haxby JV, Gobbini MI. 2011. *Distributed neural systems for face perception*. Oxford, England: Oxford University Press. <https://doi.org/10.1093/oxfordhb/9780199559053.013.0006>.
- Haxby JV, Hoffman EA, Gobbini MI. 2000. The distributed human neural system for face perception. *Trends Cogn Sci*. 4(6):223–232.
- Haxby JV, Gobbini MI, Furey ML, Ishai A, Schouten JL, Pietrini P. 2001. Distributed and overlapping representations of faces and objects in ventral temporal cortex. *Science (New York, NY)*. 293(5539):2425–2430. <https://doi.org/10.1126/science.1063736>.
- Hebb D. 1949. *The organization of behavior: a neuropsychological theory*. New York: John Will & Sons.
- Hermann P, Grotheer M, Kovács G, Vidnyánszky Z. 2017. The relationship between repetition suppression and face perception.

- Brain Imaging Behav. 11(4):1018–1028. <https://doi.org/10.1007/s11682-016-9575-9>.
- Hesse JK, Tsao DY. 2020. The macaque face patch system: a turtle's underbelly for the brain. *Nat Rev Neurosci*. 21(12):695–716. <https://doi.org/10.1038/s41583-020-00393-w>.
- Hills PJ, Lewis MB. 2018. The development of face expertise: evidence for a qualitative change in processing. *Cogn Dev*. 48:1–18. <https://doi.org/10.1016/j.cogdev.2018.05.003>.
- Horovitz SG, Rossion B, Skudlarski P, Gore JC. 2004. Parametric design and correlational analyses help integrating fMRI and electrophysiological data during face processing. *Neuro Image*. 22(4):1587–1595. <https://doi.org/10.1016/j.neuroimage.2004.04.018>.
- Huang L, Song Y, Li J, Zhen Z, Yang Z, Liu J. 2014. Individual differences in cortical face selectivity predict behavioral performance in face recognition. *Front Hum Neurosci*. 483:1–10. <https://doi.org/10.3389/fnhum.2014.00483>.
- Hung CC, Yen CC, Ciuchta JL, Papoti D, Bock NA, Leopold DA, Silva AC. 2015. Functional mapping of face-selective regions in the extrastriate visual cortex of the marmoset. *J Neurosci*. 35(3):1160–1172. <https://doi.org/10.1523/JNEUROSCI.2659-14.2015>.
- Ishai A. 2008. Let's face it: it's a cortical network. *Neuro Image*. 40(2):415–419. <https://doi.org/10.1016/j.neuroimage.2007.10.040>.
- Ishai A, Schmidt CF, Boesiger P. 2005. Face perception is mediated by a distributed cortical network. *Brain Res Bull*. 67(1–2):87–93. <https://doi.org/10.1016/j.brainresbull.2005.05.027>.
- Jiang X, Bollich A, Cox P, Hyder E, James J, Gowani SA, Hadjikhani N, Blanz V, Manoch DS, Barton JJS, et al. 2013. A quantitative link between face discrimination deficits and neuronal selectivity for faces in autism. *Neuro Image*. 2(1):320–331. <https://doi.org/10.1016/j.nicl.2013.02.002>.
- Jonas J, Rossion B. 2021. Intracerebral electrical stimulation to understand the neural basis of human face identity recognition. *Eur J Neurosci*. 54:4197–4211. <https://doi.org/10.1111/ejn.15235>.
- Jonas J, Descroins M, Koessler L, Colnat-Coulbois S, Sauvée M, Guye M, Vignal J-P, Vespignani H, Rossion B, Maillard L. 2012. Focal electrical intracerebral stimulation of a face-sensitive area causes transient prosopagnosia. *Neuroscience*. 222:281–288. <https://doi.org/10.1016/j.neuroscience.2012.07.021>.
- Jonas J, Jacques C, Liu-Shuang J, Brissart H, Colnat-Coulbois S, Maillard L, Rossion B. 2016. A face-selective ventral occipito-temporal map of the human brain with intracerebral potentials. *Proc Natl Acad Sci*. 113(28):E4088–E4097. <https://doi.org/10.1073/pnas.1522033113>.
- Julian JB, Fedorenko E, Webster J, Kanwisher N. 2012. An algorithmic method for functionally defining regions of interest in the ventral visual pathway. *Neuro Image*. 60(4):2357–2364. <https://doi.org/10.1016/j.neuroimage.2012.02.055>.
- Kanwisher N. 2017. The quest for the FFA and where it led. *J Neurosci*. 37(5):1056–1061. <https://doi.org/10.1523/JNEUROSCI.1706-16.2016>.
- Kanwisher N, McDermott J, Chun MM. 1997. The fusiform face area: a module in human extrastriate cortex specialized for the perception of faces. *J Neurosci*. 17(11):4302–4311. <http://www.ncbi.nlm.nih.gov/pubmed/9151747>.
- Kessler R, Rusch KM, Wende KC, Schuster V, Jansen A. 2021. Revisiting the effective connectivity within the distributed cortical network for face perception. *NeuroImage: Reports*. 1:100045.
- Kim JJ, Crespo-Facorro B, Andreasen NC, O'Leary DS, Zhang B, Harris G, Magnotta VA. 2000. An MRI-based parcellation method for the temporal lobe. *Neuro Image*. 11(4):271–288. <https://doi.org/10.1006/nimg.2000.0543>.
- Levy I, Hasson U, Avidan G, Hendler T, Malach R. 2001. Center-periphery organization of human object areas. *Nat Neurosci*. 4(5):533–539. <https://doi.org/10.1038/87490>.
- Loffler G, Yourganov G, Wilkinson F, Wilson HR. 2005. fMRI evidence for the neural representation of faces. *Nat Neurosci*. 8(10):1386–1390. <https://doi.org/10.1038/nn1538>.
- Logothetis NK. 2008. What we can do and what we cannot do with fMRI. *Nature*. 453(7197):869–878. <https://doi.org/10.1038/nature06976>.
- Lorenz S, Weiner KS, Caspers J, Mohlberg H, Schleicher A, Bludau S, Eickhoff SB, Grill-Spector K, Zilles K, Amunts K. 2017. Two new Cytoarchitectonic areas on the human mid-fusiform gyrus. *Cereb Cortex*. 27(1):373–385. <https://doi.org/10.1093/cercor/bhv225>.
- Malikovic A, Amunts K, Schleicher A, Mohlberg H, Eickhoff SB, Wilms M, Palomero-Gallagher N, Armstrong E, Zilles K. 2007. Cytoarchitectonic analysis of the human extrastriate cortex in the region of V5/MT+: a probabilistic, stereotaxic map of area hOc5. *Cereb Cortex*. 17(3):562–574. <https://doi.org/10.1093/cercor/bhj181>.
- Mandler G. 1980. Recognizing: the judgment of previous occurrence. *Psychol Rev*. 87(3):252–271. <https://doi.org/10.1037/0033-295X.87.3.252>.
- Margalit E, Jamison KW, Weiner KS, Vizioli L, Zhang RY, Kay KN, Grill-Spector K. 2020. Ultra-high-resolution fMRI of human ventral temporal cortex reveals differential representation of categories and domains. *J Neurosci*. 40(15):3008–3024. <https://doi.org/10.1523/JNEUROSCI.2106-19.2020>.
- Marr D. 1982. Vision: a computational investigation into the human representation and processing of visual information. [https://doi.org/10.1016/0022-2496\(83\)90030-5](https://doi.org/10.1016/0022-2496(83)90030-5)
- McCaffery JM, Robertson DJ, Young AW, Burton AM. 2018. Individual differences in face identity processing. *Cogn Res Princ Implic*. 21:1–15. <https://doi.org/10.1186/s41235-018-0112-9>.
- McCarthy G, Spicer M, Adrignolo A, Luby M, Gore J, Allison T. 1994. Brain activation associated with visual motion studied by functional magnetic resonance imaging in humans. *Hum Brain Mapp*. 2(4):234–243. <https://doi.org/10.1002/hbm.460020405>.
- McGugin RW, Ryan KF, Tamber-Rosenau BJ, Gauthier I. 2018. The role of experience in the face-selective response in right FFA. *Cereb Cortex*. 28(6):2071–2084. <https://doi.org/10.1093/cercor/bhx113>.
- Meyers EM, Borzello M, Freiwald WA, Tsao D. 2015. Intelligent information loss: the coding of facial identity, head pose, and non-face information in the macaque face patch system. *J Neurosci*. 35(18):7069–7081. <https://doi.org/10.1523/JNEUROSCI.3086-14.2015>.
- Moeller S, Freiwald WA, Tsao DY. 2008. Patches with links: a unified system for processing faces in the macaque temporal lobe. *Science*. 320(5881):1355–1359. <https://doi.org/10.1126/science.1157436>.
- Mountcastle VB. 1997. The columnar organization of the neocortex. In: *Brain* (vol. 120, Issue 4). <https://doi.org/10.1093/brain/120.4.701>
- Mueller S, Wang D, Fox MD, Yeo BTT, Sepulcre J, Sabuncu MR, Shafee R, Lu J, Liu H. 2013. Individual variability in functional connectivity architecture of the human brain. *Neuron*. 77(3):586–595. <https://doi.org/10.1016/j.neuron.2012.12.028>.
- O'Craven KM, Downing PE, Kanwisher N. 1999. fMRI evidence for objects as the units of attentional selection. *Nature*. 401(6753):584–587. <https://doi.org/10.1038/44134>.
- O'Toole AJ, Jiang F, Abdi H, Haxby JV. 2005. Partially distributed representations of objects and faces in ventral temporal cortex. *J Cogn Neurosci*. 17(4):580–590. <https://doi.org/10.1167/4.8.903>.
- Oldfield RC. 1971. The assessment and analysis of handedness: the Edinburgh inventory. *Neuropsychologia*. 9(1):97–113. [https://doi.org/10.1016/0028-3932\(71\)90067-4](https://doi.org/10.1016/0028-3932(71)90067-4).

- Orlov T, Makin TR, Zohary E. 2010. Topographic Representation of the Human Body in the Occipitotemporal Cortex. *Neuron*. 68:586–600.
- Parvizi J, Jacques C, Foster BL, Withoft N, Rangarajan V, Weiner KS, Grill-Spector K. 2012. Electrical stimulation of human fusiform face-selective regions distorts face perception. *J Neurosci*. 32(43):14915–14920. <https://doi.org/10.1523/JNEUROSCI.2609-12.2012>.
- Peelen MV, Downing PE. 2007. The neural basis of visual body perception. *Nat Rev Neurosci*. 8:636–648.
- Peelen MV, Fei-Fei L, Kastner S. 2009. Neural mechanisms of rapid natural scene categorization in human visual cortex. *Nature*. 460(7251):94–97. <https://doi.org/10.1038/nature08103>.
- Pinsk MA, DeSimone K, Moore T, Gross CG, Kastner S. 2005. Representations of faces and body parts in macaque temporal cortex: a functional MRI study. *Proc Natl Acad Sci U S A*. 102(19):6996–7001. <https://doi.org/10.1073/pnas.0502605102>.
- Pinsk MA, Arcaro M, Weiner KS, Kalkus JF, Inati SJ, Gross CG, Kastner S. 2009. Neural representations of faces and body parts in macaque and human cortex: a comparative fMRI study. *J Neurophysiol*. 101(5):2581–2600. <https://doi.org/10.1152/jn.91198.2008>.
- Pitcher D, Ungerleider LG. 2021. Evidence for a third visual pathway specialized for social perception. *Trends Cogn Sci*. 25(2):100–110. <https://doi.org/10.1016/j.tics.2020.11.006>.
- Pitcher D, Walsh V, Yovel G, Duchaine B. 2007. TMS Evidence for the Involvement of the Right Occipital Face Area in Early Face Processing. *Curr Biol*. 17:1568–1573.
- Pitcher D, Walsh V, Duchaine B. 2011. The role of the occipital face area in the cortical face perception network. In *Experimental brain research* (vol. 209, Issue 4, pp. 481–493). <https://doi.org/10.1007/s00221-011-2579-1>
- Pourtois G, Schwartz S, Seghier ML, Lazeyras F, Vuilleumier P. 2005. Portraits or people? Distinct representations of face identity in the human visual cortex. *J Cogn Neurosci*. 17(7):1043–1057. <https://doi.org/10.1162/0898929054475181>.
- Puce A, Allison T, Gore JC, McCarthy G. 1995. Face-sensitive regions in human extrastriate cortex studied by functional MRI. *J Neurophysiol*. 74(3):1192–1199. <http://www.ncbi.nlm.nih.gov/pubmed/7500143>.
- Pyles JA, Verstynen TD, Schneider W, Tarr MJ. 2013. Explicating the face perception network with white matter connectivity. *PLoS One*. 8(4):e61611. <https://doi.org/10.1371/journal.pone.0061611>.
- Quek GL, Rossion B. 2017. Category-selective human brain processes elicited in fast periodic visual stimulation streams are immune to temporal predictability. *Neuropsychologia*. 104:182–200. <https://doi.org/10.1016/j.neuropsychologia.2017.08.010>.
- Rajimehr R, Young JC, Tootell RBH. 2009. An anterior temporal face patch in human cortex, predicted by macaque maps. *Proc Natl Acad Sci*. 106(6):1995–2000. <https://doi.org/10.1073/pnas.0807304106>.
- Regan D. 1989. *Human brain electrophysiology: evoked potentials and evoked magnetic fields in science and medicine*. New York: Elsevier.
- Retter TL, Jiang F, Webster MA, Michel C, Schiltz C, Rossion B. 2021. Varying Stimulus Duration Reveals Consistent Neural Activity and Behavior for Human Face Individuation. *Neuroscience*. 472:138–156.
- Retter TL, Rossion B. 2016. Uncovering the neural magnitude and spatio-temporal dynamics of natural image categorization in a fast visual stream. *Neuropsychologia*. 91:9–28.
- Rice GE, Watson DM, Hartley T, Andrews TJ. 2014. Low-level image properties of visual objects predict patterns of neural response across category-selective regions of the ventral visual pathway. *J Neurosci*. 34(26):8837–8844. <https://doi.org/10.1523/JNEUROSCI.5265-13.2014>.
- Rosenke M, Weiner KS, Barnett MA, Zilles K, Amunts K, Goebel R, Grill-Spector K. 2017. A cross-validated cytoarchitectonic atlas of the human ventral visual stream. *Neuro Image*. 170:257–270. <https://doi.org/10.1016/j.neuroimage.2017.02.040>.
- Rosenke M, van Hoof R, van den Hurk J, Grill-Spector K, Goebel R. 2021. A probabilistic functional atlas of human occipito-temporal visual cortex. *Cereb Cortex*. 31(1):603–619. <https://doi.org/10.1093/cercor/bhaa246>.
- Rossion B. 2008. Constraining the cortical face network by neuroimaging studies of acquired prosopagnosia. *Neuro Image*. 40(2):142–158. <https://doi.org/10.1016/j.neuroimage.2007.10.047>.
- Rossion B. 2014. Understanding individual face discrimination by means of fast periodic visual stimulation. *Exp Brain Res*. 232(6):1599–1621. <https://doi.org/10.1007/s00221-014-3934-9>.
- Rossion B, Retter TL. 2020. Face perception. In: Poeppel D, Gazzaniga MS, Mangun G, editors. *The cognitive neurosciences*. 6th ed Chapter 11, pp. 129–139. Cambridge, MA: MIT Press.
- Rossion B, Taubert J. 2019. What can we learn about human individual face recognition from experimental studies in monkeys? *Vis Res*. 157. <https://doi.org/10.1016/j.visres.2018.03.012>.
- Rossion B, Schiltz C, Crommelinck M. 2003. The functionally defined right occipital and fusiform “face areas” discriminate novel from visually familiar faces. *Neuro Image*. 19(3):877–883. [https://doi.org/10.1016/S1053-8119\(03\)00105-8](https://doi.org/10.1016/S1053-8119(03)00105-8).
- Rossion B, Hanseeuw B, Dricot L. 2012. Defining face perception areas in the human brain: a large-scale factorial fMRI face localizer analysis. *Brain Cogn*. 79(2):138–157. <https://doi.org/10.1016/j.bandc.2012.01.001>.
- Rossion B, Torfs K, Jacques C, Liu-Shuang J. 2015. Fast periodic presentation of natural images reveals a robust face-selective electrophysiological response in the human brain. *J Vis*. 15(1):18–18. <https://doi.org/10.1167/15.1.18>.
- Rossion B, Jacques C, Jonas J. 2018. Mapping face categorization in the human ventral occipitotemporal cortex with direct neural intracranial recordings. *Ann N Y Acad Sci*. 1426:5–24. <https://doi.org/10.1111/nyas.13596>.
- Rottschy C, Eickhoff SB, Schleicher A, Mohlberg H, Kujovic M, Zilles K, Amunts K. 2007. Ventral visual cortex in humans: cytoarchitectonic mapping of two extrastriate areas. *Hum Brain Mapp*. 28(10):1045–1059. <https://doi.org/10.1002/hbm.20348>.
- Saxe R, Powell LJ. 2006. It’s the thought that counts: specific brain regions for one component of theory of mind. *Psychol Sci*. 17(8):692–699. <https://doi.org/10.1111/j.1467-9280.2006.01768.x>.
- Scherf KS, Luna B, Avidan G, Behrmann M. 2011. “What” precedes “which”: developmental neural tuning in face- and place-related cortex. *Cereb Cortex*. 21(9):1963–1980. <https://doi.org/10.1093/cercor/bhq269>.
- Schiltz C, Rossion B. 2006. Faces are represented holistically in the human occipito-temporal cortex. *Neuro Image*. 32(3):1385–1394. <https://doi.org/10.1016/j.neuroimage.2006.05.037>.
- Schwarz L, Kreifelts B, Wildgruber D, Erb M, Scheffler K, Ethofer T. 2019. Properties of face localizer activations and their application in functional magnetic resonance imaging (fMRI) fingerprinting. *PLoS One*. 14(4):e0214997. <https://doi.org/10.1371/journal.pone.0214997>.
- Schwarzlose RF, Swisher JD, Dang S, Kanwisher N. 2008. The distribution of category and location information across object-selective regions in human visual cortex. *Proc Natl Acad Sci*. 105:4447–4452.
- Sergent J, Ohta S, Macdonald B. 1992. Functional neuroanatomy of face and object processing a positron emission tomography study. *Brain*. 115(1):15–36. <https://doi.org/10.1093/brain/115.1.15>.

- Smith SM, Jenkinson M, Woolrich MW, Beckmann CF, Behrens TEJ, Johansen-Berg H, Bannister PR, De Luca M, Drobnjak I, Flitney DE, et al. 2004. Advances in functional and structural MR image analysis and implementation as FSL. *Neuro Image*. 23(suppl. 1):S208–S219. <https://doi.org/10.1016/j.neuroimage.2004.07.051>.
- Taubert J, Japee S, Murphy AP, Tardiff CT, Koele EA, Kumar S, Leopold DA, Ungerleider LG. 2020. Parallel Processing of Facial Expression and Head Orientation in the Macaque Brain. *J Neurosci*. 40:8119–8131.
- Taubert J, Van Belle G, Vanduffel W, Rossion B, Vogels R. 2015. Neural correlate of the thatcher face illusion in a monkey face-selective patch. *J Neurosci*. 35(27):9872–9878. <https://doi.org/10.1523/JNEUROSCI.0446-15.2015>.
- Tong F, Nakayama K, Vaughan JT, Kanwisher N. 1998. Binocular rivalry and visual awareness in human extrastriate cortex. *Neuron*. 21(4):753–759. [https://doi.org/10.1016/S0896-6273\(00\)80592-9](https://doi.org/10.1016/S0896-6273(00)80592-9).
- Tong F, Nakayama K, Moscovitch M, Weinrib O, Kanwisher N. 2000. Response properties of the human fusiform face area. *Cogn Neuropsychol*. 17(1):257–280. <https://doi.org/10.1080/026432900380607>.
- Tsantani M, Kriegeskorte N, Storrs K, Williams AL, McGettigan C, Garrido L. 2021. Ffa and ofa encode distinct types of face identity information. *J Neurosci*. 41(9):9872–9878. <https://doi.org/10.1523/JNEUROSCI.1449-20.2020>.
- Tsao DY, Moeller S, Freiwald WA. 2008. Comparing face patch systems in macaques and humans. *Proc Natl Acad Sci*. 105(49):19514–19519. <https://doi.org/10.1073/pnas.0809662105>.
- Vassal F, Pommier B, Sontheimer A, Lemaire JJ. 2018. Interindividual variations and hemispheric asymmetries in structural connectivity patterns of the inferior fronto-occipital fascicle: a diffusion tensor imaging tractography study. *Surg Radiol Anat*. 40(2):129–137. <https://doi.org/10.1007/s00276-017-1966-0>.
- Wandell BA. 2011. The neurobiological basis of seeing words. *Ann NY Acad Sci*. 1224(1):63–80. <https://doi.org/10.1111/j.1749-6632.2010.05954.x>.
- Wang Y, Metoki A, Smith DV, Medaglia JD, Zang Y, Benear S, Popal H, Lin Y, Olson IR. 2020. Multimodal mapping of the face connectome. *Nat Hum Behav*. 4(4):397–411. <https://doi.org/10.1038/s41562-019-0811-3>.
- Weibert K, Andrews TJ. 2015. Activity in the right fusiform face area predicts the behavioural advantage for the perception of familiar faces. *Neuropsychologia*. 75:588–596. <https://doi.org/10.1016/j.neuropsychologia.2015.07.015>.
- Weiner KS. 2019. The mid-fusiform sulcus (sulcus sagittalis gyri fusiformis). *Anat Rec*. 302:1491–1503. <https://doi.org/10.1002/ar.24041>.
- Weiner KS, Grill-Spector K. 2010. Sparsely-distributed organization of face and limb activations in human ventral temporal cortex. *Neuro Image*. 52(4):1559–1573. <https://doi.org/10.1016/j.neuroimage.2010.04.262>.
- Weiner KS, Grill-Spector K. 2011. Not one extrastriate body area: using anatomical landmarks, hMT+, and visual field maps to parcellate limb-selective activations in human lateral occipitotemporal cortex. *Neuro Image*. 56(4):2183–2199. <https://doi.org/10.1016/j.neuroimage.2011.03.041>.
- Weiner KS, Grill-Spector K. 2012. The improbable simplicity of the fusiform face area. *Trends Cogn Sci*. 16(5):251–254. <https://doi.org/10.1016/j.tics.2012.03.003>.
- Weiner KS, Grill-Spector K. 2015. The evolution of face processing networks. *Trends Cogn Sci*. 19(5):240–241. <https://doi.org/10.1016/j.tics.2015.03.010>.
- Weiner KS, Barnett MA, Witthoft N, Golarai G, Stigliani A, Kay KN, Gomez J, Natu VS, Amunts K, Zilles K, et al. 2017. Defining the most probable location of the parahippocampal place area using cortex-based alignment and cross-validation. *Neuro Image*. April. 1–12. <https://doi.org/10.1016/j.neuroimage.2017.04.040>.
- Worsley KJ. 2005. An improved theoretical P value for SPMs based on discrete local maxima. *Neuro Image*. 28(4):1056–1062. <https://doi.org/10.1016/j.neuroimage.2005.06.053>.
- Yovel G, Freiwald WA. 2013. Face recognition systems in monkey and human: are they the same thing? *F1000Prime Reports*. 5(April):1–8. <https://doi.org/10.12703/P5-10>.
- Yue X, Cassidy BS, Devaney KJ, Holt DJ, Tootell RBH. 2011. Lower-level stimulus features strongly influence responses in the fusiform face area. *Cereb Cortex*. 21(1):35–47. <https://doi.org/10.1093/cercor/bhq050>.
- Zhen Z, Yang Z, Huang L, Kong X, Wang X, Dang X, Huang Y, Song Y, Liu J. 2015. Quantifying interindividual variability and asymmetry of face-selective regions: a probabilistic functional atlas. *Neuro Image*. 113:13–25. <https://doi.org/10.1016/j.neuroimage.2015.03.010>.